THE JOURNAL OF BIOLOGICAL CHEMISTRY VOL. 289, NO. 32, pp. 22221–22236, August 8, 2014

Sin3b Interacts with Myc and Decreases Myc Levels*

Received for publication, December 23, 2013, and in revised form, June 9, 2014 Published, JBC Papers in Press, June 20, 2014, DOI 10.1074/jbc.M113.538744

Pablo Garcia-Sanz[‡§¶1], Andrea Quintanilla[‡], M. Carmen Lafita[‡], Gema Moreno-Bueno[§¶], Lucia García-Gutierrez[‡], Vedrana Tabor[‖2], Ignacio Varela[‡], Yuzuru Shiio[**], Lars-Gunnar Larsson[‖], Francisco Portillo[§3], and Javier Leon[‡4]

*From the [‡]Instituto de Biomedicina y Biotecnología de Cantabria (IBBTEC), Consejo Superior de Investigaciones Científicas, Universidad de Cantabria, Sociedad para el Desarrollo de Cantabria and the Departamento de Biología Molecular, Universidad de Cantabria, Santander 39011, Spain, the [§]Instituto de Investigaciones Biomédicas Alberto Sols, Consejo Superior de Investigaciones Científicas, Instituto de Investigación Hospital Universitario La Paz (IdiPaz), Facultad de Medicina, Universidad Autónoma de Madrid, 28046 Madrid, Spain, the [¶]Fundación M. D. Anderson Internacional, Madrid, Spain, the [‖]Department of Microbiology, Tumor and Cell Biology, Karolinska Institute, Stockholm SE-17177, Sweden, and the **Greehey Children's Cancer Research Institute, The University of Texas Health Science Center, San Antonio, Texas 78229-3900*

Background: Myc is an oncogenic transcription factor that is frequently deregulated in cancer, and Sin3b is a transcriptional regulator that recruits histone deacetylases.
Results: A new interaction between the protein Sin3b and Myc that leads to Myc down-regulation is described.
Conclusion: Sin3b-Myc interaction regulates Myc levels and activity.
Significance: Sin3b adds a second level of control of Myc by directly regulating Myc levels.

Myc expression is deregulated in many human cancers. A yeast two-hybrid screen has revealed that the transcriptional repressor Sin3b interacts with Myc protein. Endogenous Myc and Sin3b co-localize and interact in the nuclei of human and rat cells, as assessed by co-immunoprecipitation, immunofluorescence, and proximity ligation assay. The interaction is Max-independent. A conserved Myc region (amino acids 186–203) is required for the interaction with Sin3 proteins. Histone deacetylase 1 is recruited to Myc-Sin3b complexes, and its deacetylase activity is required for the effects of Sin3b on Myc. Myc and Sin3a/b co-occupied many sites on the chromatin of human leukemia cells, although the presence of Sin3 was not associated with gene down-regulation. In leukemia cells and fibroblasts, Sin3b silencing led to Myc up-regulation, whereas Sin3b overexpression induced Myc deacetylation and degradation. An analysis of Sin3b expression in breast tumors revealed an association between low Sin3b expression and disease progression. The data suggest that Sin3b decreases Myc protein levels upon Myc deacetylation. As Sin3b is also required for transcriptional repression by Mxd-Max complexes, our results suggest that, at least in some cell types, Sin3b limits Myc activity through two complementary activities: Mxd-dependent gene repression and reduction of Myc levels.

c-Myc (hereafter Myc) is an oncogenic transcription factor of the helix-loop-helix/leucine zipper protein family. Myc forms heterodimers with the protein Max, which bind to DNA sequences called E-boxes (1–3). Myc-Max regulates thousands of genes and binds to about 15% of genomic loci. Most target genes are activated by Myc in an E-box-dependent manner, although an important fraction of Myc target genes are repressed (4–7). Recent developments suggest that Myc functions as an amplifier of active genes (8, 9) Myc activates transcription by recruiting a multiprotein complex that includes histone acetyltransferases (2, 10, 11). In agreement with its large number of target genes, Myc exerts a wide array of biological functions including cell cycle control, genomic instability, energetic metabolism, protein synthesis, intercellular communication, and control of cell differentiation (1, 10, 12, 13). Myc is deregulated in about half of human tumors and frequently appears to be associated with tumor progression (14–16).

Myc transcriptional activity is also controlled by several competing repressive Max-binding partners of the Mxd family (Mxd1, Mxi1, Mxd3, Mxd4, and Mnt). Mxd-Max dimers are biochemical antagonists of Myc-Max, *i.e.* they repress gene expression upon binding to E-boxes in the regulatory regions of the target genes (17, 18). Mxd-Max heterodimers repress transcription by recruiting Sin3a and Sin3b. Sin3 originally was discovered in yeasts as an essential component of transcriptional regulatory complexes containing multiple components (19, 20). Mammalian Sin3 proteins were discovered as interactors of Mxd proteins, which carry a conserved Sin3-interacting domain (SID) in their N-terminal region (21–24). Sin3-Mxd interaction takes place through the paired amphipathic helices (PAH)[5] of the Sin3a/b C-terminal region and is required for the transcriptional repression exerted by Mxd proteins on their

* This work was supported by Grants SAF11-23796 from the Ministerio de Economía y Competitividad (MINECO) and RETIC/RD012/0036/0033 from the Instituto Carlos III (to J. L.); SAF2010-20175 from MINECO, AECC-2011 from the Asociación Española Contra el Cáncer (AECC), and ReCaRe S2010/BMD-2303 from Comunidad de Madrid (to G. M.-B.); and BFU2008-04285 from MINECO (to F. P.). All Spanish funding, except from the AECC, was co-sponsored by the European Union Fondo de Desarrollo Regional de la Unión Europea (FEDER) program.
[1] Recipient of a fellowship from the Formación de Profesorado Universitario (FPU) program, Spanish Ministry of Education.
[2] Supported by grants from the Cancerfonden and the Karolinska Institutet. Present address: Dept. of Medical Biochemistry and Biophysics, Karolinska Inst., Stockholm SE-17177, Sweden.
[3] To whom correspondence may be addressed. Tel.: 34-914-972732; Fax: 34-914-975353; E-mail: fportillo@iib.uam.es.
[4] To whom correspondence may be addressed. Tel.: 34-942-201952; Fax: 34-942-266399; E-mail: leonj@unican.es.

[5] The abbreviations used are: PAH, paired amphipathic helices; HDAC, histone deacetylase; TPA, 12-*O*-tetradecanoylphorbol-13-acetate; TSA, trichostatin A; isPLA, *in situ* proximity ligation assay; UCSC, University of California, Santa Cruz; RPKM, reads per kb per million mapped reads; RT-qPCR, reverse transcription-quantitative polymerase chain reaction.

target genes (22, 25–27). The mechanism through which Sin3b represses transcription involves the recruitment of histone deacetylases (HDACs) types 1 and 2 (28–30). Sin3-containing complexes, besides HDAC1 and HDAC2, contain other proteins to form a transcription regulatory complex (reviewed in Refs.19, 29, and 31). Compared with Sin3a interactions, much less is known about Sin3b interactions. There are differences in the protein interactions described for each Sin3 family member (32–35) and the phenotypes of Sin3a- and Sin3b-deficient mice, with the Sin3a knock-out mice showing an earlier lethality than Sin3b knock-out mice (35). Here we show an interaction between Myc and Sin3b that results in impaired Myc transcriptional activity. The Myc region involved in the interaction is a small conserved region (Myc box III). Myc-Sin3b interaction leads to Myc deacetylation and destabilization, and co-expression of Sin3b leads to reduced Myc levels.

EXPERIMENTAL PROCEDURES

Breast Tumor Samples and Immunohistochemical Analysis—A total of 106 infiltrating ductal breast carcinoma tumors from the archive of the Pathology Department of the M. D. Anderson Cancer Center (Madrid, Spain) were studied. All of the tumors were grade 3. Patients underwent surgery between 2006 and 2007. The mean patient age at surgery was 57.8 years (range, 33 to 82 years). According to the TNM (tumor-node-metastasis) classification for staging, 32 of the tumors were stage I, 35 were stage II, and 34 were stage III–IV. Among the tumors, 17.5% developed metastasis. Histological and immunohistochemical studies were all carried out on formalin-fixed, paraffin-embedded tissue samples. The standard ethical procedures of the Spanish regulation (Ley de Investigación Biomédica) were followed. All participants in this study signed informed consent forms, and the study was approved by the Institutional Review Boards and the bioethics committee of the M. D. Anderson Cancer Center (Madrid, Spain). Sin3b immunohistochemical staining was performed by the labeled streptavidin-biotin (EnVision™+ kits, Dako) method with a heat-induced antigen retrieval step. Briefly, sections were immersed in boiling 10 mM sodium citrate, pH 6.0, for 3 min in a pressure cooker. A polyclonal antibody against human Sin3b was used. The antibodies used are listed in Table 1. The primary antibodies were omitted in the negative controls. Sin3b staining was scored as positive when nuclear localization was observed in at least 10% of the tumor cells and as negative when expressed in less than 10% of the tumor cells. For the meta-analysis of breast cancer and Sin3b correlation, the breast microarray and clinical data were obtained from the International Cancer Research (ICR) database. The statistical survival analysis of breast samples was performed using ROCK and SPSS software. Kaplan-Meier plots were used to estimate the overall survival curves using log-rank tests. The expression value of Sin3b was categorized using the upper quartile (25%) against the rest. The chi-square contingency test with Yates' correction or a Fisher's exact test was used to determine the statistical significance of the relationships between *SIN3B* expression and survival or metastasis. Values of $p < 0.05$ were considered statistically significant. These analyses were carried out using the SPSS 17.0 software.

Yeast Two-hybrid Screening—The Matchmaker system 3 (Clontech) was used for the yeast two-hybrid screen. The bait protein consisted of the full-length human Myc protein subcloned in the pGBKT7 vector (containing a GAL4 DNA-binding domain). A pACT2 vector-based mouse NIH3T3 fibroblast cDNA library (Mouse Embryonic Fibroblast Matchmaker, Clontech) was used to screen for prey proteins. Yeasts (AH109 strain) were transformed with the EasyComp transformation kit for *Saccharomyces cerevisiae* (Invitrogen). Positive colonies were isolated based on their capacity to express the markers ADE2 and HIS3, which allowed them to grow on SC −AHLW, a selection medium lacking tryptophan, leucine (selection markers for pGBKT7 and pACT2 plasmids, respectively), adenine, and histidine. pTD1 and pVA3 plasmids (Clontech) were used as an interaction positive control in the yeast two-hybrid system. The pLAM5′ plasmid (Clontech) was used as a control to detect fortuitous protein-protein interactions. pACT2-Myc vector consisted of full-length human Myc subcloned in the pACT2 vector, which encodes for the GAL4 transactivation domain. The clones were also grown in SC −LW medium, which lacks tryptophan and leucine (the selection markers for pGBKT7- and pACT2-based plasmids, respectively), to rule out the possibility that the absence of growth in the selection medium SC −AHLW was not due to an inefficient transformation.

Cell Culture and Transfections—HEK293T and K562 cells were from ATCC. K562/S is a K562 subclone able to grow attached to plastic (36). The P493-6 cell line consists of immortalized human B cells carrying a tetracycline-repressible Myc transgene (37). K562 cells and derivatives were grown in RPMI medium (Invitrogen) supplemented with 10% fetal bovine serum (Lonza), 100 units/ml penicillin, and 100 μg/ml streptomycin. Rat1a cells were a gift from Chi Dang (University of Pennsylvania) (38). Rat1aMyc was generated by transfection of Rat1a cells with pCEFL-Myc (36) and selection with 0.4 mg/ml G418 (Sigma). UR61 cells derive from rat pheochromocytoma (39). Rat1a and UR61 cells were cultured in DMEM (Invitrogen) supplemented with serum and antibiotics as described above. The vectors used were as follows: pME18S-Myc-FLAG, pME18S-MycD1–98-FLAG, pME18S-MycD106–143-FLAG, pME18S-MycD157–262-FLAG, pME18S-MycD186–203-FLAG, pME18S-MycD244–271-FLAG, and pME18S-MycD348–439-FLAG (39). pcDNA3-Myc-HA was constructed in this work, using the Myc cDNA from pCEFL-Myc (36). pcDNA3-Sin3b-FLAG and pcDNA3-Sin3b-HA were constructed from pcDNA3-Sin3b, encoding full-length murine Sin3b cDNA (a gift from Gregory David, New York University Medical Center, NY). Other vectors used for transfections were: pcDNA3-HDAC1-FLAG, pcDNA3-HDAC2-FLAG, and pSC2-Sin3a-myc (22) and the corresponding empty vectors pME18S, pcDNA3, pCEFL, and pSC2. For transient transfection of HEK293T cells for protein immunoprecipitation and immunoblot analysis, typically 750,000 cells were transfected using FuGENE 6 transfection reagent (Roche Applied Science) following the manufacturer's instructions and were lysed 24 h after transfection. In order to silence Sin3b expression in Rat1aMyc cells and in K562 cells, two siRNA duplexes (Mission siRNA, Sigma-Aldrich, 100 pmol each; RNA sequences available upon request) were transfected to each cell line by using

TABLE 1

Primary antibodies used

Use in immunoblot (IB), immunofluorescence (IF), immunoprecipitation (IP), proximity ligase assay (PLA), immunohistochemistry (IHQ), and chromatin immunoprecipitation (ChIP) experiments is indicated. The dilution of the antibodies used for immunoblot was 1:1000.

Antigen	Type	Source	Reference no.	Use (dilution)
Acetyl-lysine	Mouse monoclonal	Cell Signaling Technology	9681	IB
Actin	Goat polyclonal	Santa Cruz Biotechnology	I-19, sc-1616	IB
FLAG	Mouse monoclonal	Sigma-Aldrich	F3165	IB, IP
GST	Rabbit polyclonal	Sigma-Aldrich	G7781	IB
HDAC1	Rabbit polyclonal	Abcam	Ab19845	IB
HA	Rat monoclonal	Roche Applied Science	3F10	IB, IP
Max	Rabbit polyclonal	Santa Cruz Biotechnology	C124, sc-765	PLA (1:100)
Mxd1	Rabbit polyclonal	Santa Cruz Biotechnology	C19, sc-222	PLA (1:100)
Myc	Mouse monoclonal	Santa Cruz Biotechnology	C33, sc-42	PLA (1:25) IB
	Mouse monoclonal	Santa Cruz Biotechnology	9E10, sc-40	IB
	Mouse Monoclonal	Neomarkers	Ab5, MS-1054	IB
	Rabbit polyclonal	Santa Cruz Biotechnology	N-262, sc-764	IB, IP, ChIP IF (1:100) PLA (1:50)
Kat2A	Goat polyclonal	Santa Cruz Biotechnology	N-18, sc-6303	IB
Phospho-H3 (Ser-10)	Rabbit polyclonal	Santa Cruz Biotechnology	sc-8656	IB
Sin3b	Rabbit polyclonal	Santa Cruz Biotechnology	A20, sc-996	IB, IP, ChIP IF (1:200) IHQ (1:100) PLA (1:100)
	Mouse monoclonal	Santa Cruz Biotechnology	H4, sc-13145	IB
α-Tubulin	Rabbit polyclonal	Santa Cruz Biotechnology	H-300, sc-5546	IB

TABLE 2

Sequences of the PCR primers used

The forward primer is listed first, and the reverse primer is listed second. All primers were used at 0.3 μM.

Gene (species)	Primer sequences 5′ → 3′	Used for
β-Actin (human)	AAATCTGGCACCACACCTTC and TAGCACAGCCTGGATAGCAA	RT-qPCR
CAD (human)	CCGCAGTCTCTGCTGCTG and ACCCGTCCTCCAACACTAGG	ChIP
CDK4 (human)	CTGACCGGGAGATCAAGGTA and GGCTTCAGATCTCGGTGAAC	RT-qPCR
	AGGCATGTGTCATGTGTGATCTT and CCGCTCCCAGTCTTCCTTG	ChIP
HES1 (human)	CGGACATTCTGGAAATGACA and GTGCGCACCTCGGTATTAAC	RT-qPCR
	GGCAATAAAACATCCTGGCAC and TCATCCGTAGGCTTTAGGTTCTG	ChIP
LDHA (human)	TCCTGACTCAGGCTCATG and AGACAACCGACCGGCAGA	ChIP
MYC (human)	AAGACTCCAGCGCCTTCTCT and GTTTTCCAACTCCGGGATCT	RT-qPCR
RPS14 (human)	CAAGGGGAAGGAAAAGAAGG and GAGGACTCATCTCGGTCAGC	RT-qPCR
SIN3B (rat)	CATCCAGTCACCTCTGAGCA and GATCTCAGGGTGGTCCAGAA	RT-qPCR
SRD5A1 (human)	AAAGCCTATGCCACTGTTGG and ACATGCCCGTTAACCACAAG	RT-qPCR
	GAAACCAAGGCCCCACGT and TGCGCTTTGGGCTTATTCC	ChIP

Lipofectamine 2000 (Invitrogen) for Rat1aMyc and by electroporation in an Amaxa electroporator for K562 cells. Sin3b RNA levels were analyzed 24 h after transfection. K562 cells were transiently transfected with 5 μg of pcDNA3-Sin3bHA plasmid or empty pCDNA3 vector. When indicated, the cells were treated with 12-*O*-tetradecanoylphorbol-13-acetate (TPA, Sigma), trichostatin A (TSA, Sigma), and vorinostat (from LC Biochemicals).

Protein Analysis—Cells were lysed using cold lysis buffer consisting of 1% IGEPAL (Sigma-Aldrich), 150 mM NaCl, 50 mM Tris, pH 8, and 1 mM EDTA, pH 8, and the following protease and phosphatase inhibitors: aprotinin (20 μg/ml), leupeptin (2 μg/ml), PMSF (2 mM), sodium orthovanadate (1 mM), sodium fluoride (5 mM) and β-glycerol phosphate (5 mM). The protein concentration was determined using the BCA assay (Thermo Scientific). For protein immunoprecipitation, typically 300 μg of protein was immunoprecipitated with 1 μg of the corresponding antibody using protein G-coupled Dynabeads magnetic beads (Dynal, Invitrogen). Mouse IgG was from Jackson ImmunoResearch Laboratories. For immunoblotting, the entire immunoprecipitated fraction (for co-immunoprecipitation analysis) or 50 μg of protein (for expression analysis) was electrophoresed in SDS-PAGE (acrylamide percentage ranging from 7.5 to 10%) and transferred onto PVDF or nitrocellulose membranes (Millipore) by standard procedures. The primary antibodies used are shown in Table 1. Immunoblots were revealed with an enhanced chemiluminescence system (GE Healthcare) or with the Odyssey scanner (LI-COR Biosciences).

RNA Analysis—Total RNA was isolated using the RNeasy mini kit (Qiagen). cDNAs preparation by reverse transcription and quantitative polymerase chain reaction (RT-qPCR) was performed as described previously (40). The primers for the assayed genes are shown in Table 2. The expression of the analyzed genes was normalized against the β-actin mRNA levels.

Pull-down Assay—For the pull-down assay, DH5α cells (Invitrogen) were transformed with pGEX-Myc-GST (glutathione *S*-transferase) plasmid (41) and grown to exponential phase at 37 °C until an $A_{600\,nm}$ of 0.6–0.8 was reached. Myc-GST expression was induced with 0.5 mM IPTG for 3 h at 37 °C. The cell pellet was resuspended in BFX buffer (20 mM Tris, pH 7.4, 1 M NaCl, 0.2 mM EDTA, 1% Triton X-100, and protease-phosphatase inhibitors) and sonicated. After centrifugation (13,000 rpm for 30 min), the supernatant was collected and incubated for 1 h at 4 °C with glutathione-Sepharose 4B beads (GE Healthcare) equilibrated previously with PBS and BFX buffer. Beads were washed with GST-FISH buffer (10% glycerol, 50 mM Tris, pH 7.4, 100 mM NaCl, 1% Nonidet P-40, and 2 mM $MgCl_2$) and

incubated for 2 h at 4 °C with a protein extract obtained from HEK293T cells transfected with pcDNA3-Sin3b-HA (and the corresponding pcDNA3 vector) 24 h earlier. After four washes with GST-FISH buffer, the proteins were collected and analyzed by immunoblotting. For the GST-Sin3b and recombinant Myc pull-down assay, the first 1170 nucleotides (390 amino acids) of murine Sin3b cDNA were subcloned into pGEX-4T vector (GE Healthcare). This region encompasses the first three PAH domains at the N terminus of the protein (NSin3b). To this end, pcDNA3-Sin3b was digested with BamHI and the resultant fragment subcloned in the pGEX-4T vector, generating the pGEX-4T-Sin3b plasmid. Myc recombinant protein was purchased from OriGene. DH5α cells (Invitrogen) were transformed with pGEX-4T-Sin3b (and the corresponding empty vector) and grown to exponential phase at 37 °C until an $A_{600\,nm}$ of 0.6–0.8 was reached. GST-Sin3b expression was induced with 0.5 mM IPTG for 3 h at 37 °C. The cell pellet was resuspended in BFX buffer and sonicated. After centrifugation (13,000 rpm for 30 min), the supernatant was collected and incubated for 1 h at 4 °C with Pierce glutathione magnetic beads (Thermo Scientific), previously equilibrated with binding/wash buffer (125 mM Tris, pH 8, and 150 mM NaCl). Beads were washed with binding/wash buffer and incubated for 2 h at 4 °C with 50 ng of Myc recombinant protein. After three washes with binding/wash buffer, the beads were resuspended in Western blot loading buffer (containing SDS and β-mercaptoethanol) and boiled at 95 °C for 5 min, and the supernatant fractions (containing the proteins) were collected and analyzed by immunoblotting.

Luciferase Reporter Assays—The luciferase reporters used were as follows: pGL3-E-box, carrying four E-box elements in the pGL3 vector; and pGL3-E-BoxMut, carrying four mutated E-boxes (42). Cells were transfected using FuGENE 6 transfection reagent (Roche Applied Science) with 30 ng of the reporter vector, 3 ng of the pCMVβ vector (Clontech) encoding β-galactosidase (Clontech), and a total amount of 200 ng of the indicated expression vectors. Twenty-four hours after transfection, cells were lysed and luciferase activity measured with the luciferase assay substrate from the Dual-Luciferase reporter assay system (Promega). The activity of firefly luciferase was normalized to that of β-galactosidase used as an internal control. To this end, β-galactosidase activity was measured using the Beta-Glo assay system (Promega). For treatment with the HDAC inhibitors, cells transfected with the reporter and expression vectors were treated 24 h after transfection with 300 nM TSA or 5 μM vorinostat for another 24 h after luciferase activity was measured. The statistical significance of the differences between luciferase values was based on p values calculated using the Student's t test.

Immunofluorescence and in Situ Proximity Ligation Assay (isPLA)—For immunofluorescence experiments, K562/S cells were grown on coverslips and treated with 20 nM TPA (Sigma) when indicated. Twenty-four hours after treatment, the cells were fixed for 15 min in 3.7% paraformaldehyde in PBS. Then the cells were permeabilized with 0.5% Triton X-100 for 30 min, blocked for 30 min at 37 °C in 3% BSA/PBS/0.01Triton X-100, incubated with primary antibodies overnight at 4 °C, washed in PBS, and incubated with secondary antibodies. Subsequently, samples were blocked in rabbit serum (Santa Cruz Biotechnology, sc-2338) for 1 h and incubated again with primary and secondary antibodies. After several washes, the cells were mounted in mounting medium with DAPI (Invitrogen). The primary antibodies are listed in Table 1. The secondary antibodies were donkey anti-rabbit 488 and goat anti-rabbit 555 (Alexa Fluor, both diluted at 1:500). For isPLA we essentially followed the technique already described (43). K562/S cells grown on coverslips were treated with TPA, fixed, and permeabilized as above. The cells were incubated with blocking solution for 2 h at 37 °C and then incubated with primary antibodies dissolved in blocking buffer (100 mM L-cysteine, 0.1 μg/ml salmon sperm DNA, 0.5 M EDTA, 0.05% Tween 20, 30 and μg/ml BSA in PBS) for 16 h at 4 °C. For each interaction a pair of mouse and rabbit primary antibodies was used. The antibodies and dilutions are listed in Table 1. To assay the Myc-Sin3b interaction, we used anti-Myc rabbit polyclonal antibody and anti-Sin3b mouse monoclonal antibody. To detect the primary antibodies, secondary proximity probes binding rabbit and mouse immunoglobulin (PLA® probe anti-rabbit PLUS and PLA probe anti-mouse MINUS, Olink Bioscience) were diluted at 1:15 and 1:5, respectively, in blocking solution. The slides were incubated with this proximity probe solution for 1 h at 37 °C, washed three times in 50 mM Tris, pH 7.6, 150 mM NaCl, and 0.05% Tween-20 (TBS-T), and incubated with hybridization solution containing connector oligonucleotides (Olink Bioscience) for 45 min at 37 °C. Then the samples were washed with TBS-T and subsequently incubated in the ligation solution for 45 min at 37 °C. The ligation solution contained T4 DNA ligase (Fermentas), allowing the ligation of secondary proximity probes and connector oligonucleotides to form a circular DNA strand. Subsequently, the samples were washed in TBS-T, incubated with the amplification solution containing phi29 DNA polymerase (Fermentas) for the roller cycle amplification for 90 min at 37 °C, and washed three times with TBS-T. Finally, the samples were incubated with detection mix solution (containing Texas Red-labeled detection probes that recognize the amplified product; Olink Bioscience) for 1 h at 37 °C, washed twice in SSC-T buffer (150 mM NaCl, 15 mM sodium citrate, and 0.05% Tween 20, pH 7) and ethanol, and then mounted. Fluorescence signals were detected by laser-scanning microscopy (Axiovert 200M, Zeiss) and analyzed with AxioVision software (Zeiss). isPLA-positive signals were quantified using ImageJ software. At least 200 nuclei were measured for each experimental condition.

Chromatin Immunoprecipitation (ChIP)—Cells were fixed with 1% formaldehyde for 10 min at room temperature, and fixation was stopped by incubation with 0.12 M glycine for 10 min at room temperature. The cells were washed with PBS and lysed in 1% SDS lysis buffer. Cross-linked chromatin was fragmented by sonication to an average size of 500 bp and immunoprecipitated (500,000 cells/antibody). Antibodies and cell lysates were incubated overnight at 4 °C and then for 4 h at 4 °C with protein G-coupled magnetic beads (Dynabeads, Invitrogen) blocked with salmon sperm DNA (1 h at 4 °C). The protein-DNA cross-link was reversed in elution buffer (1% SDS and 0.1 M $NaHCO_3$) and RNase overnight at 65 °C. The eluted material was treated with proteinase K for 3 h at 45 °C, and the DNA

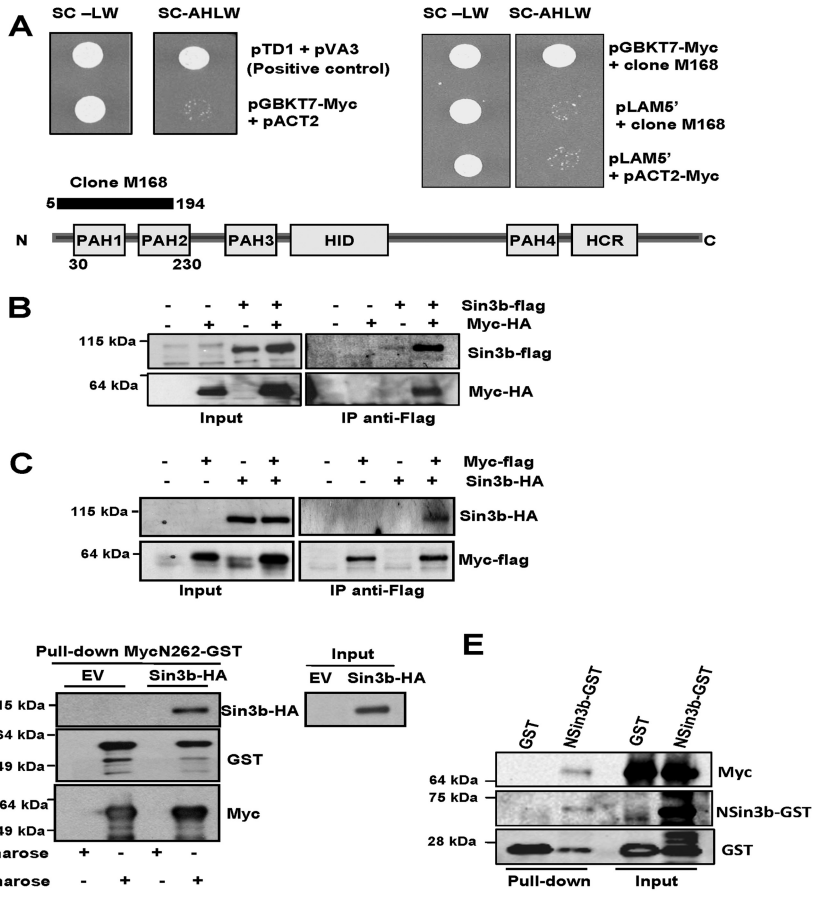

FIGURE 1. **Sin3b and Myc interact.** *A*, interaction between Myc and Sin3b detected in two-hybrid screen. *S. cerevisiae* AH109 yeast was transformed with expression vectors, indicated at the *right*, and plated on selection media SC −LW and SC −AHLW as indicated. The *left panel* shows the positive and Myc controls, indicating that Myc does not allow growth in the restriction medium by itself. The *right panel* shows the growth due to the interaction of Myc with the protein encoded by clone M168. The region of Sin3b protein encoded by the M168 clone is shown at the *bottom*. The *right panel* also shows that Myc does not interact with lamin C, a control used to detect fortuitous or unspecific protein interactions. *B*, co-immunoprecipitation (*IP*) of Myc and Sin3b in HEK293T cells. The cells were transfected with vectors for Myc-HA and Sin3b-FLAG, and after transfection, the lysates were immunoprecipitated with anti-FLAG to detect Sin3b-bound proteins. The immunoprecipitates were analyzed by immunoblotting with anti-FLAG and anti-HA antibodies as indicated. Immunoprecipitations with immunoglobulin G were conducted as a negative control (not shown). *C*, the cells were transfected with vectors encoding Myc-FLAG and Sin3b-HA, and after transfection, the lysates were immunoprecipitated with anti-FLAG to detect Myc-bound proteins. The immunoprecipitates were analyzed by Western blotting as in *B*. *D*, cellular Sin3b binds to recombinant Myc. Bacterially expressed Myc-GST was mixed with lysates of HEK293T cells transfected with pCDNA3-Sin3b-HA or empty vector (*EV*). Myc-GST was incubated with glutathione-Sepharose, and the pulled down material was analyzed by immunoblotting with the indicated antibodies. Sin3b expression in the input lysates is shown at the *right*. *E*, recombinant Sin3b and Myc proteins interact *in vitro*. A fusion protein consisting of GST and the N-terminal domain of murine Sin3b (first 390 amino acids (*NSin3b*)) and Myc purified protein were incubated with glutathione bound to magnetic beads. The levels of Myc, GST-NSin3b, and GST were determined in the inputs and in the pulled down material by immunoblotting.

was purified using the QIAquick PCR purification kit (Qiagen). Quantitative PCR (SYBR Green PCR kit, Bio-Rad) was performed in a Bio-Rad iCycler iQ5 apparatus. The immunoprecipitations were carried out with anti-Myc and anti-Sin3b antibodies or nonimmune rabbit IgG as a negative control (Table 1). The signals were normalized to the inputs and the signals obtained with the non-immune rabbit IgG immunoprecipitation. The re-ChIP assays were performed as described above until reversion of protein-DNA cross-links. Magnetic beads were eluted by using SDS elution buffer with 10 mM DTT for 1 h at 37 °C. Half of the anti-Myc-immunoprecipitated chromatin was then incubated with anti-Sin3B (A-20, Santa Cruz Biotechnology.) antibody; the other half was incubated with non-immune IgG (Santa Cruz Biotechnology) as a control overnight at 4 °C. The subsequent steps were carried out as described above. The data are the mean values ± S.E. of two independent experiments. The primers are listed in Table 2.

Genome-wide Chip-seq Analysis—DNA binding sites for Sin3a and Max proteins in the K562 cell line identified by the ENCODE/HAIB project were downloaded from the University of California, Santa Cruz (UCSC), database. Similarly, DNA binding sites for the c-Myc protein in K562 and GM12878 cell lines identified by the ENCODE/Open Chrom project (release of September 2012) were downloaded from the UCSC database. In order to restrict the analysis to only *bona fide* binding sites, in the case of Sin3a and Max, only those binding sites present in both technical replicates were used. In the case of Myc, binding sites from two human hematopoietic cell lines (K562 and GM12878) were compared and the analysis was restricted to the common binding sites. To detect those binding sites present in gene promoters, gene information from the RefSeq database was downloaded from the UCSC database (GRCh37/hg19 RefSeq release 55), and information 1 kb upstream and downstream of the transcription starting site for each gene (as anno-

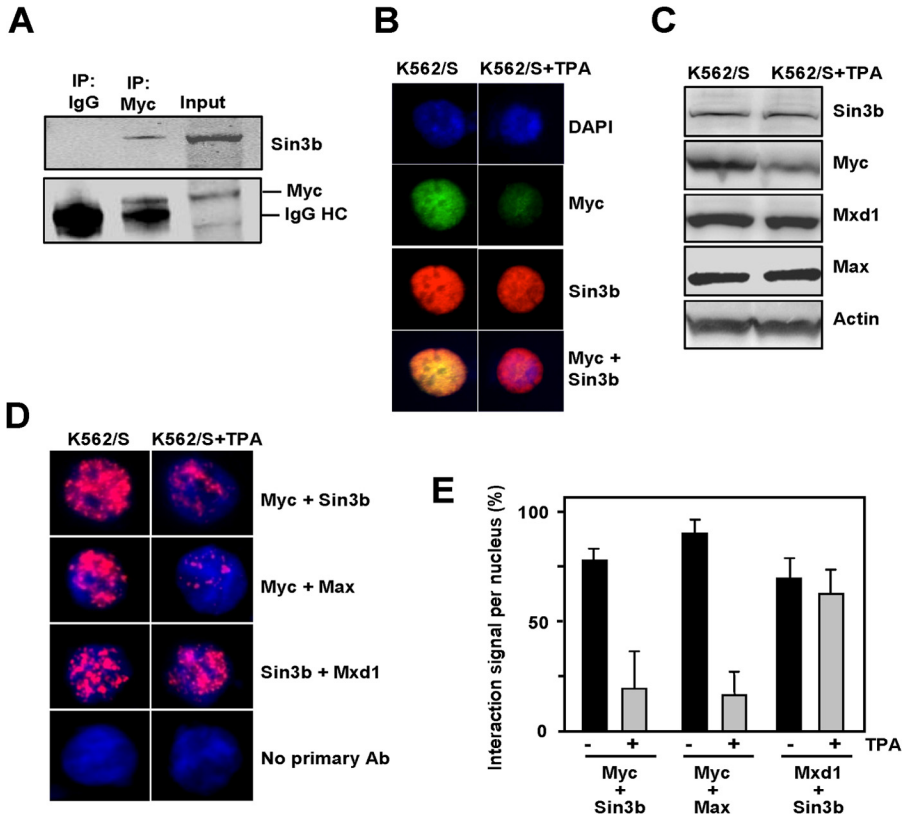

FIGURE 2. **Interaction between endogenous Myc and Sin3b.** *A*, endogenous Myc and Sin3b interact in the nuclei of human cells. Lysates from K562/S cells were immunoprecipitated (*IP*) with anti-Myc antibodies as indicated, and the levels of Sin3b and Myc were analyzed by immunoblotting. *IgG HC*, rabbit heavy chain IgG cross-reacting with anti-murine IgGs. *B*, immunofluorescence of the indicated proteins in K562/S cells untreated and treated with TPA to decrease Myc expression. Confocal images of the nuclei of representative cells are shown. In the *bottom panel* (Myc + Sin3b), the *yellow color* indicates co-localization of Sin3b and Myc in the nucleus. *C*, immunoblot of Myc, Sin3b, Mxd1, and Max proteins in K562/S cells untreated and treated with 10 nM TPA for 24 h. *D*, detection of Myc-Sin3b interaction by *in situ* PLA. A representative nucleus is shown for each pair of interactive proteins assayed. Nuclei were counterstained with DAPI. The anti-Sin3b and anti-Myc antibodies used were rabbit A20 and mouse C33 antibodies, respectively (Table 1). *E*, quantification of isPLA signals. At least 200 nuclei were scored for each pair of assayed proteins. 100% means that the positive signal covered the entire nucleus.

tated in the UCSC browser) was extracted. All downloaded files were homogenized to bed format using perl and awk scripts written in-house (available upon request). Finally, all comparisons between the number of binding sites of different proteins were performed using the intersectBed tool from the BedTools suite (44). A minimum of 10% of sequence overlap between different binding sites was required. The normalization of binding sites/Mb was estimated considering 51.3 Mb of total promoter sequence (according to RefSeq) and 3 Gb of total genomic sequence. RNA-seq BAM files from ENCODE/Caltech corresponding to two non-strand-specific RNA 75-bp paired-end experiments in the K562 cell line were downloaded from the UCSC database. RPKM (reads per kb per million mapped reads) were calculated using Cufflinks v2.0.2, and the mean of the two replicates were used for forward analysis. Only genes with Myc, Sin3a, or both in their promoter (defined as above) and with expression levels of >5 RPKM were selected. Accumulated frequencies were normalized against the number of expressed genes in each case and plotted against the RPKM.

RESULTS

Sin3b Identified as a Myc Interactor in a Yeast Two-hybrid Assay—To identify new Myc interactors, the ORF of human Myc was used as bait in a two-hybrid assay in *S. cerevisiae* AH109 strain. The vector pGBKT7-Myc was co-transformed with a NIH3T3 library based on the pACT2 vector. pGBKT7-Myc with empty vector did not give positive colonies (Fig. 1*A*, *left*). Also, the co-transformation of pACT2-Myc and pLAM5′ (which encodes for lamin C) did not allow growth in restriction medium (Fig. 1*A*, *right*), indicating that the positive clones obtained in the screening were not artifacts due to fortuitous interactions. Sixty positive clones (*i.e.* growing in selective medium SC −AHLW) were detected in our screens. We focused on one of them, clone M168, which encoded a region of Sin3b, a transcriptional co-repressor known to interact with Mxd proteins. The region of clone M168 comprised amino acids 5–194 of the mouse Sin3b protein (Fig. 1*A*). This region of Sin3b encompasses the PAH1 domain (amino acids 30–100) and part of the PAH2 domain (amino acids 145–230) (Fig. 1*A*, *bottom panel*). Next, we confirmed this interaction in animal cells. Expression vectors for tagged Myc and full-length Sin3b were transfected into HEK293T cells, and the lysates were immunoprecipitated for Sin3b and Myc using antibodies against the corresponding tags. The results showed that Myc was present in the immunoprecipitates for Sin3b (Fig. *1B*), and Sin3b was present in the immunoprecipitates for Myc (Fig. 1*C*). The results of the two-hybrid assay indicated a direct interaction between Myc and Sin3b. To confirm this finding, extracts of HEK293T cells transfected with Sin3b were incubated with

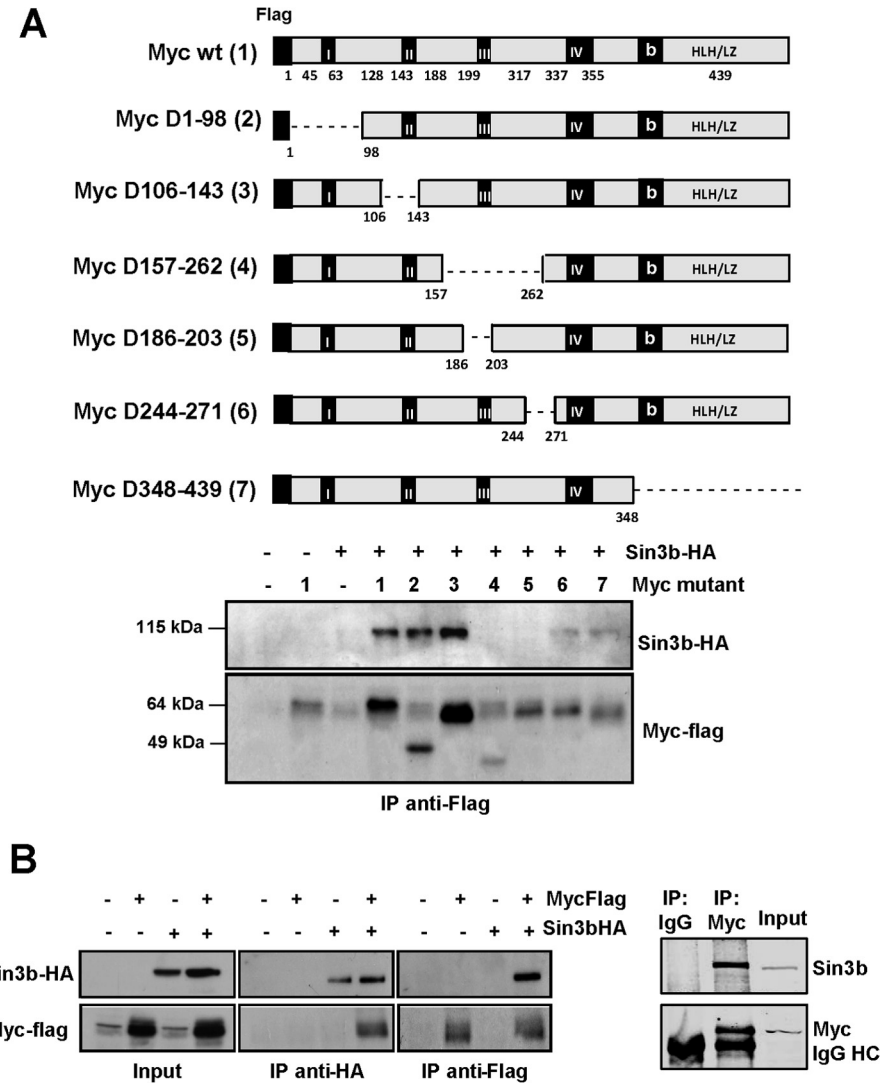

FIGURE 3. **Myc region involved in Sin3b interaction.** *A*, *upper panel*, the Myc deletion constructs used. *Lower panel*, HEK293T cells were transfected with the indicated construct and Sin3b-HA. Twenty-four hours later, Myc was immunoprecipitated (*IP*) using anti-FLAG antibody, and the presence of Sin3b in the precipitates was assayed by immunoblotting. *B*, Max is not required for Myc-Sin3b interaction. *Left panel*, UR61 cells were transfected with vectors for Myc-FLAG and Sin3b-HA, and after transfection, the lysates were immunoprecipitated with anti-FLAG. The presence of Myc and Sin3b in the immunoprecipitates was analyzed by immunoblotting with anti-FLAG and anti-HA antibodies, respectively. Immunoprecipitations with IgG were conducted as a negative control. *Right panel*, endogenous Myc of UR61 cells was immunoprecipitated with anti-Myc antibodies, and the levels of Sin3b and Myc in the immunoprecipitates were analyzed by immunoblotting. *IgG HC*, rabbit heavy chain IgG cross-reacting with anti-murine IgGs.

full-length Myc-GST recombinant protein purified from bacteria. After pull-down, Sin3b was readily detected as bound to Myc (Fig. 1*D*). Finally, we assayed the binding between recombinant Myc and Sin3b proteins. The results showed that a fusion protein consisting of GST and the three first PAH domains of Sin3b (termed GST-NSin3b) could pull down Myc protein (Fig. 1*E*). The GST protein, used as a control, did not bind Myc in this experiment. These results support the hypothesis of a direct interaction between Myc and Sin3b.

Interaction between Endogenous Myc and Sin3b Proteins—We next asked whether endogenous Myc and Sin3b interacted in the cells. We selected for this purpose human myeloid leukemia cells K562, as they are known to express high levels of Myc and also high levels of endogenous Sin3b. We conducted immunoprecipitation with anti-Myc, and Sin3b was detected in the Myc immunoprecipitates (Fig. 2*A*). The results showed that at least a fraction of endogenous Myc and Sin3b proteins interacted in K562 cells. Most of Myc and Sin3b localized in the cell nuclei, and the expectation would be that the Myc-Sin3b complexes would also be nuclear. By immunofluorescence we showed that Myc and Sin3b co-localized in the cell nuclei of K562/S cells (an adherent K562 subline) (Fig. 2*B*). The total expression of Myc and Sin3b was assessed by immunoblot (Fig. 2*C*). As a control, we used cells treated for 24 h with 20 nM TPA, a treatment that reduces Myc expression (45). To confirm the interaction between endogenous Myc and Sin3b and the cell compartment in which the interaction took place, we performed isPLA in K562/S cells. This technique allows the visualization of interactions of endogenous proteins and their localization in the cell, avoiding possible artifacts caused by protein overexpression or protein misfolding as in the FRET technique (43, 46). We used rabbit anti-Sin3b and mouse anti-Myc primary antibodies and secondary antibodies conjugated to probe oligonucleotides. The bound secondary antibodies guided the

formation of circular DNA strands when bound in close proximity. The circular DNA strands in turn served as templates for localized rolling-circle amplification, allowing the visualization of Myc-Sin3b complexes. We conducted isPLA in growing cells and in TPA-treated cells. As positive controls we also tested the interaction between Myc and Max and between Mxd1 and Sin3b. The expression of Mxd1 in these cells was assessed by immunoblotting (Fig. 2*C*). The results showed a clear positive isPLA signal in the nuclei of the cells. This signal was dramatically reduced in those cells in which Myc levels were abated by TPA treatment (Fig. 2*D*). Quantification of the corresponding signals is shown in Fig. 2*E*. Consistent with the lower Myc expression in TPA-treated cells, the level of interaction was also reduced in these cells. In contrast, the signal of Sin3b-Mxd1 was consistent with the lack of effect of TPA on Sin3b and Max levels (Fig. 2, *B* and *C*). Overall, the results demonstrated that endogenous Myc and Sin3b interact in the cell nuclei.

Myc Interacts with Sin3b through Myc Box III—The data from the yeast two-hybrid assay suggested that Sin3b interacted with Myc through the first two PAH domains (Fig. 1). To dissect the Myc regions involved in the interaction with Sin3b, we transfected HEK293T cells with Sin3b and a collection of six Myc mutants (Fig. 3*A*, *upper panel*) and conducted co-immunoprecipitations to identify the mutants with bound Sin3b. The results (Fig. 3*A*, *lower panel*) showed that the mutants MycD157–262 and MycD186–203 did not bind to Sin3b. Therefore, we concluded that the region comprising amino acids 186–203 was required for the interaction. The mutant lacking the helix-loop-helix/leucine zipper domain, which is responsible for the interaction with Max, was able to interact with Sin3b. To confirm that the interaction was independent of Max, we conducted the immunoprecipitation in PC12-derived UR61 cells, which lack a functional Max gene, expressing instead a truncated and rearranged Max (39, 47). Expression vectors for tagged Myc and Sin3b were transfected into UR61 cells, and after the immunoprecipitation of the protein lysate with anti-FLAG (for Myc) and anti-HA (for Sin3b), the presence of both proteins in the immunoprecipitated fraction was investigated by immunoblotting. The results showed that Myc and Sin3b co-immunoprecipitate in UR61 cells (Fig. 3*B*). Endogenous Myc and Sin3b of UR61 cells also co-immunoprecipitated (Fig. 3*B*, *right panel*). Overall, these results confirmed that Max was not required for Myc to interact with Sin3b.

Sin3b Antagonizes Myc Transactivation Activity—Sin3b functions as a transcriptional repressor through a mechanism involving recruitment of HDACs. Therefore, we tested whether Sin3b modified the transcriptional activity of Myc. We performed luciferase assays using a reporter carrying a minimal promoter with four Myc-binding E-boxes upstream of the luciferase gene. As a control reporter, we used the same Myc-responsive reporter construct but with mutated E-boxes, which are unable to bind to Myc-Max. The results showed that co-expression of Sin3b clearly reduced transactivation of the promoter by Myc in HEK293T cells (Fig. 4*A*).

We then studied the effect of Sin3b on the transactivation elicited by wild-type Myc and the Myc mutant MycD186–203, which is unable to bind to Sin3b. The results showed that although the MycD186–203 mutant activated the luciferase

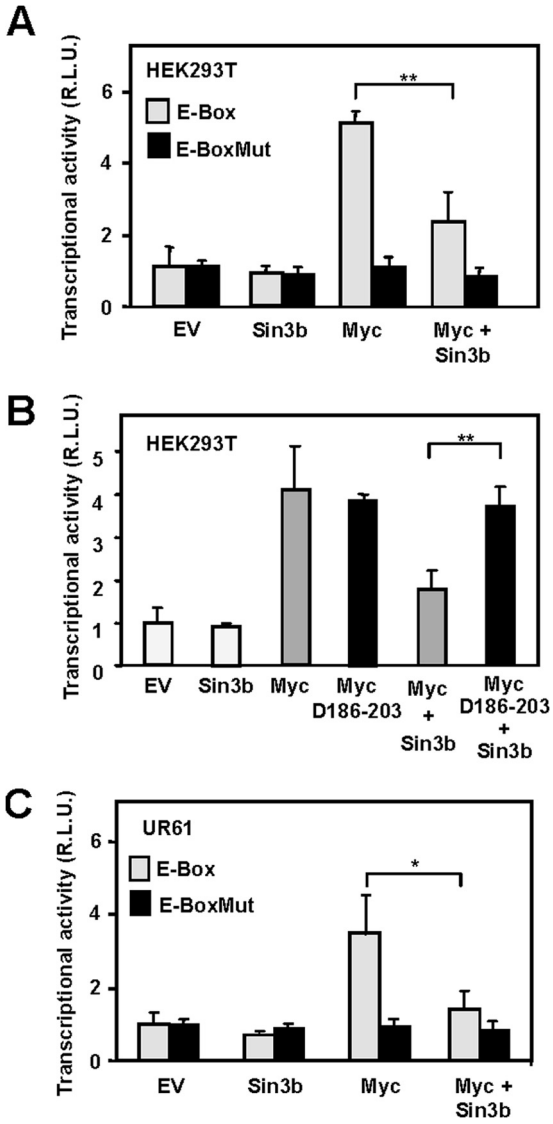

FIGURE 4. **Sin3b impairs the transactivation activity of Myc.** *A*, HEK293T cells were transfected with the indicated vectors or empty vector (*EV*). Twenty-four hours after transfection, the effect of Sin3b on Myc transcriptional activity was analyzed by a luciferase assay using a promoter-luciferase construct containing four Myc-responsive elements (*light grey*) or mutated Myc elements (*black bars*). Data were normalized to the β-galactosidase activity. Data are mean values ± S.E. of eight independent experiments. **, $p < 0.01$. *B*, HEK293T cells were transfected with the indicated Myc and Sin3b constructs, and luciferase activity was assayed as in *A*. Data are mean values ± S.E. of six independent experiments. **, $p < 0.01$. *C*, UR61 cells were transfected with the indicated vectors, and Myc transcriptional activity was determined as in *A*. Data are mean values ± S.E. values of six independent experiments. *, $p < 0.05$.

reporter to a similar extent as wild-type Myc, Sin3b was unable to impair transactivation by the Myc mutant (Fig. 4*B*), suggesting that direct interaction was required for the repression of Myc transcriptional activity by Sin3b. The results described above indicated that the Myc mutant lacking the Max interaction domain could still bind to Sin3b. To investigate whether Max was required for Sin3b-induced impairment of Myc transactivation activity, we carried out luciferase assays in the UR61 cell line. It was reported previously that Myc activates this reporter construct in the absence of Max in UR61 cells (39). We showed that Sin3b

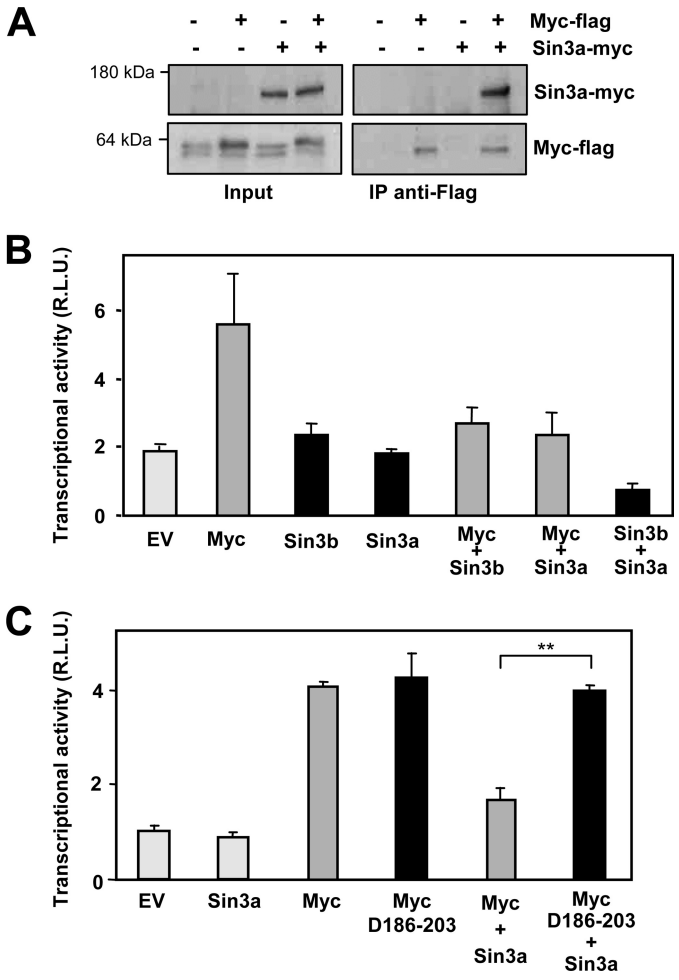

FIGURE 5. **Sin3a also binds Myc and impairs Myc transcriptional activity.** *A*, co-immunoprecipitation of Myc and Sin3a in HEK293T cells. The cells were transfected with vectors for Myc-FLAG and Sin3a-myc, and after transfection the lysates were immunoprecipitated (*IP*) with anti-FLAG to detect Myc-bound proteins. The immunoprecipitates were analyzed by immunoblotting with anti-FLAG (to detect Myc) and anti-Myc (to detect both Sin3a and Myc) antibodies. Only the band corresponding to Sin3a-myc is shown. Immunoprecipitation experiments with IgG were conducted as negative control. *B*, HEK293T cells were transfected with the indicated vectors or the empty vector (*EV*). Twenty-four hours after transfections the effect of Sin3a on Myc transcriptional activity was analyzed by a luciferase assay using a promoter-luciferase construct containing four Myc-responsive elements. Data were normalized to the β-galactosidase activity. Data are mean values ± S.E. of three independent experiments and were measured in duplicates. *C*, the Myc-(186–203) region is required for Sin3a-mediated repression. HEK293T cells were transfected with the indicated vectors or empty vector and the E-box luciferase reporter. 24 h after transfection the Myc transcriptional activity was analyzed as described in the legend for Fig. 4. Data are mean values ± S.E. of six independent experiments. **, $p < 0.01$.

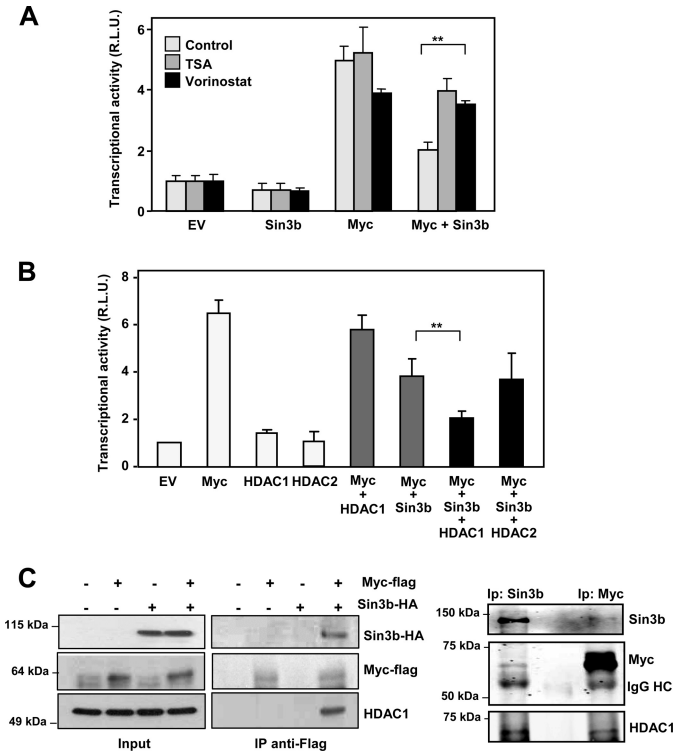

FIGURE 6. **HDAC is recruited to Myc-Sin3b complexes.** *A*, HEK293T cells were transfected with the indicated vectors or empty vector (*EV*). Twenty-four hours after transfection, the cells were treated with 0.3 μM TSA or 5 μM vorinostat for 24 h, and Myc transcriptional activity was determined by a luciferase assay using the E-box promoter construct. Data are mean values ± S.E. of six independent experiments. **, $p < 0.01$. *B*, Sin3b is required for HDAC1-mediated repression. HEK293T cells were transfected with the indicated vectors or empty vector, and Myc transcriptional activity was analyzed as described in the legend for Fig. 4. *C*, *left panel*, co-immunoprecipitation of Myc and HDAC1 in HEK293T cells. The cells were transfected with vectors for Myc-FLAG and Sin3b-HA, and after transfection, the lysates were immunoprecipitated (*IP*) with anti-FLAG. The immunoprecipitates were analyzed by immunoblotting to detect Myc, Sin3b, and HDAC1. Immunoprecipitation experiments with IgG were conducted as a negative control (not shown). *Right panel*, lysates from K562/S cells were immunoprecipitated with anti-Sin3b and anti-Myc antibodies as indicated, and the levels of Sin3b, Myc, and HDAC1 were analyzed by immunoblotting. *IgG HC*, rabbit heavy chain IgG cross-reacting with anti-murine IgG.

efficiently impaired Myc-dependent transactivation in UR61 cells, *i.e.* in the absence of Max (Fig. 4*C*).

Sin3a Also Binds Myc—We then investigated whether Myc also bound to Sin3a, the other member of the Sin3 family. We transfected Myc and Sin3a expression vectors into HEK293T cells, and co-immunoprecipitation assays were carried out as described above. The results showed that Myc also formed complexes with Sin3a (Fig. 5*A*). We compared the effects of Sin3a and Sin3b on Myc-mediated transactivation. The results of the luciferase assays indicated that Sin3a and Sin3b were similarly efficient in reducing the transcriptional activity of Myc (Fig. 5*B*). Further, similar to Sin3b, Sin3a showed no effect on the transcriptional activity of the MycD186–203 mutant (Fig. 5*C*), suggesting that the 186–203 region of Myc was responsible not only for Sin3b but also Sin3a binding.

Histone Deacetylase Also Is Recruited by Sin3b-Myc Complexes—As described in the Introduction, Sin3 proteins are known transcriptional repressors, and the mechanism of action involves the recruitment of HDACs to induce a less active chromatin conformation. To find out whether the activity of HDACs was involved in the decrease of the transcriptional activity of Myc, we first used the HDAC inhibitors TSA and vorinostat. In the presence of these inhibitors, Sin3b was unable to repress Myc activity (Fig. 6*A*). To confirm the involvement of the HDACs, we asked whether the forced expression of HDACs enhanced the repressive effect of Sin3b on Myc transcriptional activity. The cells were co-transfected with Myc, Sin3b, HDAC1, and HDAC2. We found that co-expression of HDAC1 augmented the repression exerted by Sin3b (Fig. 6*B*). In view of these results, we investigated whether HDAC1 was present in the Myc-Sin3b complexes. Co-immunoprecipitation experi-

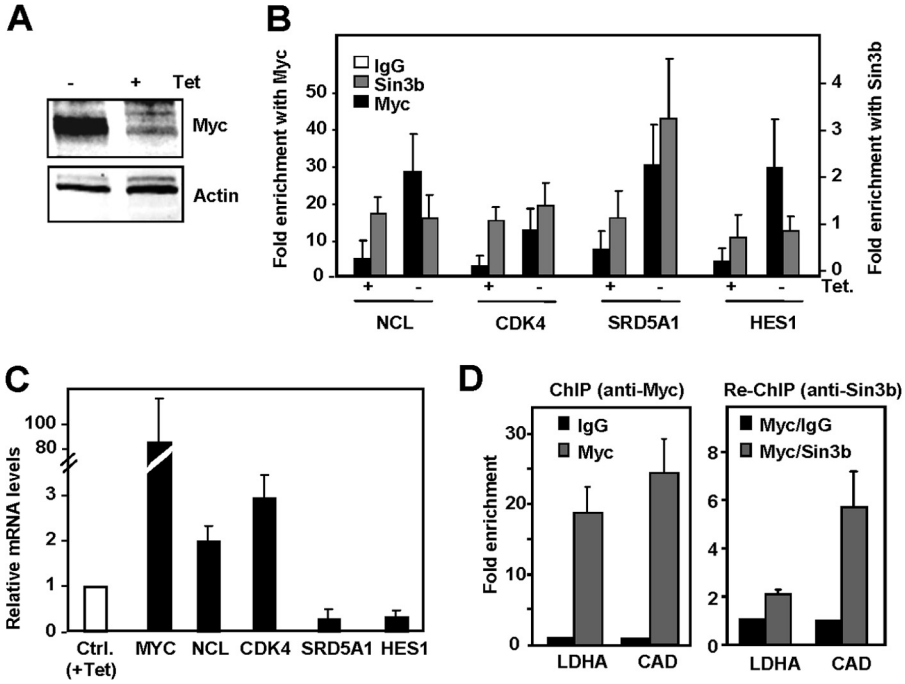

FIGURE 7. **Co-localization of Myc and Sin3b in chromatin.** *A*, repression of Myc expression by tetracycline in P493-6 cells. Cells were treated for 24 h with 0.1 μg/ml tetracycline (*Tet*), and the levels of Myc were determined by immunoblot. *B*, ChIP of Myc and Sin3b on the E-box-containing regions of *NCL*, *CDK4*, *SRD5A1*, and *HES1* genes (39). P493-6 cells were treated with tetracycline for 72 h and then washed, and grown in medium without tetracycline for another 12 h to induce Myc expression. The data are mean values of five experiments normalized against the values obtained with IgG for each amplicon. *C*, mRNA expression of the indicated genes in cells with induced Myc (*black bars*) *versus* uninduced cells. Cells were treated as described in *B*. *D*, co-occupancy of Myc and Sin3b on DNA assayed by re-ChIP. ChIP for Myc (*left panel*) and sequential ChIP for Sin3b of Myc-bound chromatin (*right panel*) were performed on the E-box-containing regions of the promoters of *CAD* and *LDHB* genes of K562 cells. Data are mean values of two independent experiments.

ments were performed in HEK293T cells, and the results showed that HDAC1 was present in the complexes with Sin3b and Myc (Fig. 6*C*, *left panel*). Moreover, endogenous HDAC1 co-immunoprecipitated with both endogenous Myc and Sin3b in K562/S cells (Fig. 6*C*, *right panel*).

Myc and Sin3 Co-localize on Chromatin—As an important fraction of Myc in the cell nuclei is bound to chromatin, we asked whether Sin3 can also be found at Myc-bound chromatin sites. Therefore we employed ChIP assays to analyze Myc-Sin3b co-localization on some Myc target sites. We used the P493-6 human lymphoblastoid cell line, which displays conditional Myc expression with the Tet-off system (37) (Fig. 7*A*). The ChIP assays, conducted on several E-box-containing promoter regions described previously as binding Myc (48), showed that Sin3b could also co-localize with Myc on the chromatin corresponding to regions of the promoter of the four genes tested (Fig. 7*B*). Interestingly we found that both Myc and Sin3b bound to the promoters regardless of whether the gene was induced (*e.g. CDK4* and *NCL*) or repressed (*e.g. SRD5A1* and *HES1*) by Myc, indicating that the extent of co-localization varies among genes but occurs both in Myc-induced (*CDK4*) and Myc-repressed genes (*SRD5A1*) (Fig. 7*C*). Indeed, in a majority of the genes tested, the ChIP Sin3b signal did not significantly increase even though Myc signal increased. To study whether Myc and Sin3a/b are in the same complex in the cells, we performed sequential ChIP (re-ChIP). Chromatin of K562 cells was first immunoprecipitated with anti-Myc antibody and then with anti-Sin3b. The results showed that Sin3b co-localized with Myc on the E-box-containing promoter region of *CAD* and *LDHB*, two typical Myc target genes (Fig. 7*D*).

Moreover, the genome-wide pattern of Myc and Sin3a (but not Sin3b) binding in several human cell lines has been determined by ChIP-seq by the ENCODE project consortium (data available at the University of California Santa Cruz browser). The comparison of Myc and Sin3a binding patterns on K562 cell line revealed that Sin3a is present in ~20% of the Myc binding sites on the genome (Fig. 8*A*). Mxd proteins may also recruit Sin3a to the same sites, and thus the actual fraction of Sin3a bound to Myc-binding regions is unknown. To assess whether the Myc-Sin3a co-localization on chromatin was higher in promoters (defined as 1 kb upstream and downstream from the transcription start site of the genes), we quantified the binding sites normalized to Mb of genomic DNA. The results show that this co-occupancy also occurred in promoters, although the sites with Myc without Sin3a were more frequent (Fig. 8*B*). Taken together, the results strongly suggest that a fraction of Myc bound to chromatin also interacts with Sin3a. Interestingly, the coincidence of Myc and Sin3a in the proximal promoters does not correlate with a lower expression with respect to genes with Myc alone (Fig. 8*C*).

Sin3b Deacetylates Myc and Promotes Myc Degradation—The fact that we did not find correlation between the presence of Sin3a/b and transcriptional repression by Myc in most genes led us to the hypothesis that the major effect of Sin3-HDAC binding was not at the level of transcriptional repression. Myc has been shown to be acetylated, which regulates Myc stability (49–52). On the other hand, it has been reported that Sin3a induces deacetylation of Myc protein resulting in decreased Myc stability (53). We asked whether this was also the case with Sin3b. HEK293T cells were transfected with expression vec-

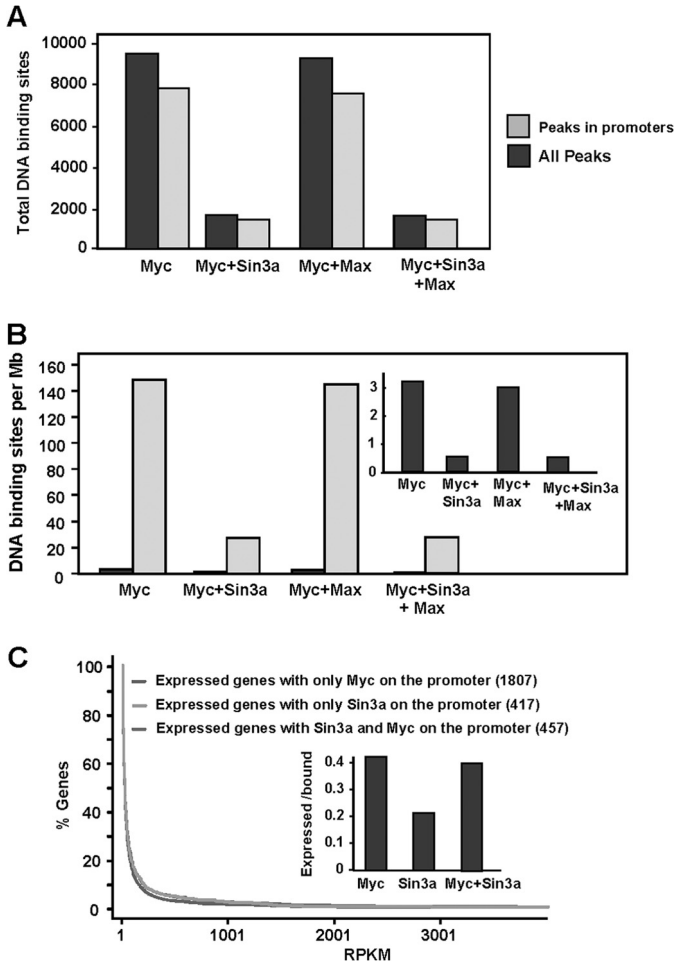

FIGURE 8. **Genomic-wide analysis of co-localization of Myc and Sin3a on chromatin of K562 cells.** *A*, binding sites in the genome of K562 cells shared by Myc, Max, and Sin3a. The *black bars* indicate the total sites (*All Peaks*) and the *gray bars* the number of sites in the promoter, defined as 1 kb upstream and downstream of the transcription start site. *B*, the number of binding sites of the indicated proteins, normalized to Mb of genomic DNA. *Black* and *gray bars* are as described in *A*. The *inset* shows only the peaks in the promoters. *C*, correlation between gene expression and binding of Myc and Sin3a to the sites in promoters of K562 cells. The graph shows the RPKM from the RNA-Seq data against the percentage of expressed genes normalized for each immunoprecipitated protein. The accumulated frequencies were normalized against the number of expressed genes in each case (shown in *parentheses*). The *inset* represents the fraction of expressed genes of those with Myc or Sin3a on their promoters.

tors for Myc, Sin3b, and the acetyltransferase Kat2a (GCN5), and 24 h after transfection the levels of acetylated Myc were assessed by immunoblot with anti-acetyl-Lys in the immunoprecipitates obtained with anti-Myc. The results showed that Kat2a expression resulted in Myc acetylation, as reported previously (53), and that levels of acetylated Myc dramatically decreased upon the expression of Sin3b (Fig. 9*A*). Consistently, transient transfection of the Sin3b expression vector into human leukemia cells (K562 and HEK293T) resulted in a reduction of Myc protein levels (Fig. 9*B*). This reduction was not observed at the Myc mRNA levels, as shown in Fig. 9*C*. We also ruled out a lower Myc protein expression due to reduced proliferation of cells transfected with Sin3b, as shown by cell counting (not shown) and by the levels of phospho-histone H3 (Fig. 9*B*). Next, we evaluated the effect of Sin3b depletion on Myc levels. The reduction of Sin3b levels upon transfection of siRNAs in human K562 cells or Rat1a fibroblasts resulted in the up-regulation of Myc protein (Fig. 9*D*). We asked whether the deacetylation of Myc mediated by Sin3b-HDAC modified the stability of Myc protein. HEK293T cells were co-transfected with Sin3b and Kat2a expression vectors, and the protein stability was assayed with cycloheximide treatment. The immunoblot results showed a faster Myc degradation in Sin3b-expressing cells (Fig. 9*E*). Altogether, the data suggest that HDAC1 is recruited to Myc-Sin3b complexes, which leads to the deacetylation and subsequent destabilization of Myc.

Low Sin3b Correlates with Breast Cancer Progression—The expression of Sin3b is reduced in many cancer types and most clearly in breast cancer (ONCOMINE database and Ref. 54). Moreover, the meta-analysis of Sin3b mRNA expression in data sets available in public breast carcinoma database showed that low Sin3b expression was associated with a decrease in overall free survival and in distant metastasis-free survival Table 3 and Fig. 10*A*). These observations, along with the above results, prompted us to explore the correlation between Sin3b and Myc protein levels in breast cancer. We analyzed Sin3b and Myc expression by immunohistochemistry in 102 infiltrating ductal breast carcinomas. We observed a lack of expression of Sin3b in 57% of the samples. Interestingly, we detected a strong association between low Sin3b expression in the primary tumors and distant metastasis (Fig. 10*B*). These observations indicated that Sin3b expression could be considered as a prognosis marker in breast cancer. In addition, we found that tumors with high Sin3b expression showed a tendency to present low Myc protein levels, although the association was weak (55.8% Myc-low *versus* 44.2% Myc-high, $p = 0.06$).

DISCUSSION

We have described here a direct interaction between Myc and the transcriptional corepressor Sin3b. We initially discovered this interaction by yeast two-hybrid screening. Furthermore, Myc and Sin3b co-immunoprecipitated in human HEK293T and rat UR61 cells upon transfection of expression vectors. Endogenous Myc and Sin3b also interacted in K562 cells, as shown by co-immunoprecipitation and isPLA. Moreover, we also detected the interaction of Sin3b with purified recombinant Myc, and we confirmed this interaction using purified Myc protein and a purified fusion Sin3b protein consisting of GST and the N-terminal region of Sin3b. Interestingly, in a previous report on two-hybrid screen designed to search Sin3b interacting peptides, two interacting peptides were found with a sequence similar to Myc Box III (55) (not shown). Although Sin3a did not appear in our initial two-hybrid screen, Sin3a also co-immunoprecipitated with Myc in cells and exerted the same effects on Myc-dependent transcription as did Sin3b. We also showed that Sin3b and Myc bind to the same promoter regions. Also, the genome-wide ChIP-seq data available in the UCSC genome browser reveal that Sin3a and Myc co-localize in a relevant fraction of chromatin sites. Taken together, the data strongly argue in favor of a direct interaction between Myc and Sin3b.

The Sin3b region found in the two-hybrid positive clone corresponds to amino acids 5–194, encompassing most of the

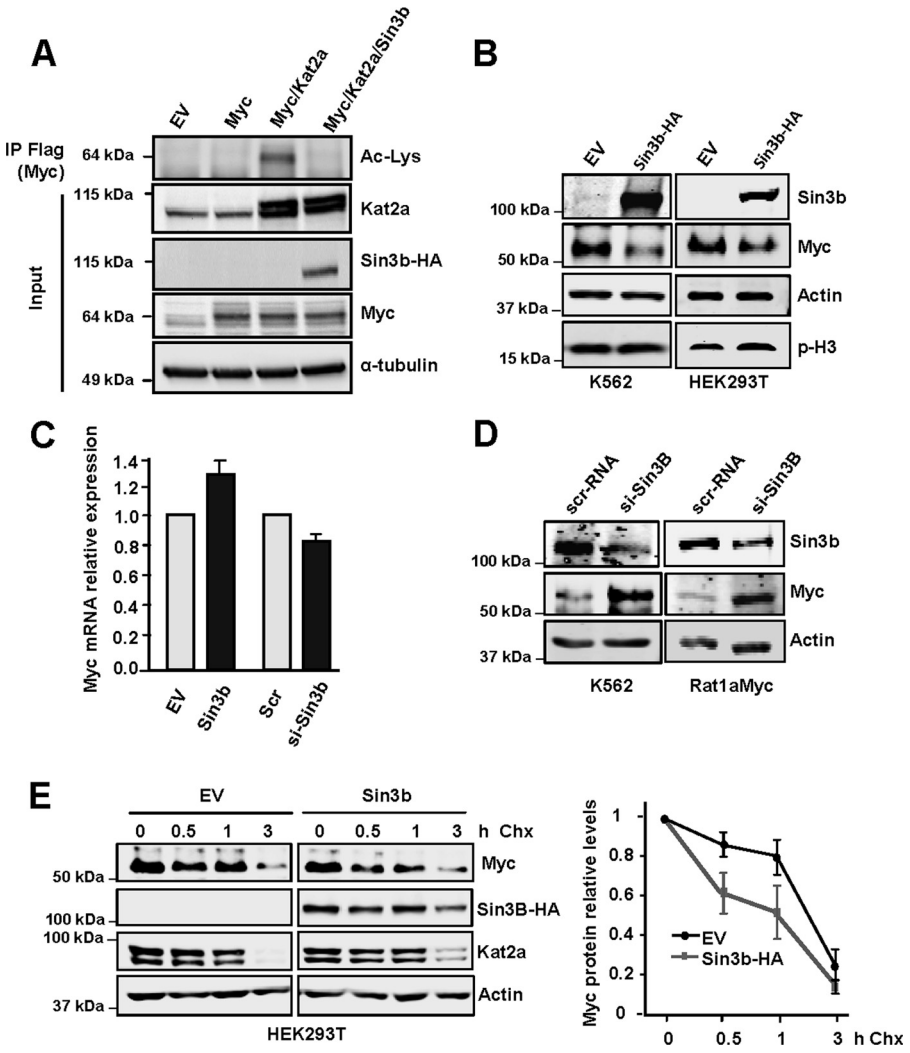

FIGURE 9. **Sin3b results in Myc deacetylation and Myc down-regulation.** *A*, HEK293T cells were transfected with Myc-FLAG, Sin3b-HA, and Kat2a expression vectors or empty vector (*EV*). Twenty-four hours after transfection, the lysates were immunoprecipitated (*IP*) with anti-FLAG antibody and analyzed by immunoblotting with anti-acetyl-lysine antibody. Levels of Myc, Kat2a, Sin3b, and α-tubulin (as loading control) in the lysates (*Input*) were determined by immunoblotting. *B*, *left panel*, K562 cells were transfected with Sin3b expression vector or empty vector, and 48 h later the levels of Sin3b, Myc, phospho-histone H3 (*p-H3*) (as a control for proliferation) and actin (as loading control) were determined by immunoblotting using mouse monoclonal antibodies for Sin3b and rabbit polyclonal antibodies for Myc and actin. Untransfected cells were also included as a control. *C*, K562 cells were transfected with Sin3b expression vector or empty vector or transfected with siRNA for Sin3b (*si-Sin3b*, 1 μg) or control scrambled siRNA. Forty-eight h later (for Sin3b expression vector transfection) or 72 h later (for siRNA-Sin3b) the levels of Myc mRNA were determined by RT-qPCR. The data were normalized to the levels of β-actin mRNA. *D*, K562 or Rat1aMyc cells were transfected with siRNA for Sin3b or scrambled siRNA as a control. Forty-eight h later, the levels of Sin3b and Myc were determined by immunoblotting. Actin was used as control for protein loading. *E*, *left panel*, HEK29T cells were transfected with Kat2a and Sin3b-HA or its corresponding empty vector, and 48 h later the cells were treated with cycloheximide (*Chx*, 60 μg/ml) for the indicated periods of time. The levels of Sin3b, Kat2a, and actin (as loading control) were determined by immunoblotting. A representative immunoblot is shown. *Right panel*, relative Myc protein levels determined by densitometry of the immunoblots. Myc signals were normalized to those of actin. Data are mean values ± S.E. from three independent experiments.

TABLE 3

Correlation of Sin3b expression with breast cancer survival and metastatic capacity

The breast microarray and clinical data were obtained from the International Cancer Research database. Several independent data sets of breast carcinoma series were analyzed. A statistical survival analysis of breast samples was performed using ROCK and SPSS software. The results corresponding to three studies are shown.

Breast cancer data set source	Low expression of Sin3b correlated to decreased overall survival[a]	Low expression of Sin3b correlated to decreased distant metastasis-free survival[a]
Van de Vijer *et al.* (59)	0.026	0.032
Perreard *et al.* (60)	0.041	0.021
Chin *et al.* (58)	0.036	0.001

[a] Log-rank test.

PAH1 and PAH2 domains (amino acids 30–230). Myc mutational analysis showed that the Sin3b-interacting region includes amino acids 186–203. This region essentially corresponds to the conserved Myc Box III (56). Interestingly, Max is not required for Sin3b binding to Myc, and Sin3b impaired Myc transcriptional activity on E-box-carrying promoters. However, Sin3b and Sin3a showed no effect on the transactivation mediated by the Myc mutant lacking the region required for Sin3 interaction (amino acids 186–203).

It has been reported that Myc represses some genes through the recruitment of HDACs and that Myc Box III is required for this activity (57). We found that the Myc region involved in this repression was the same region required for Sin3b and Sin3a

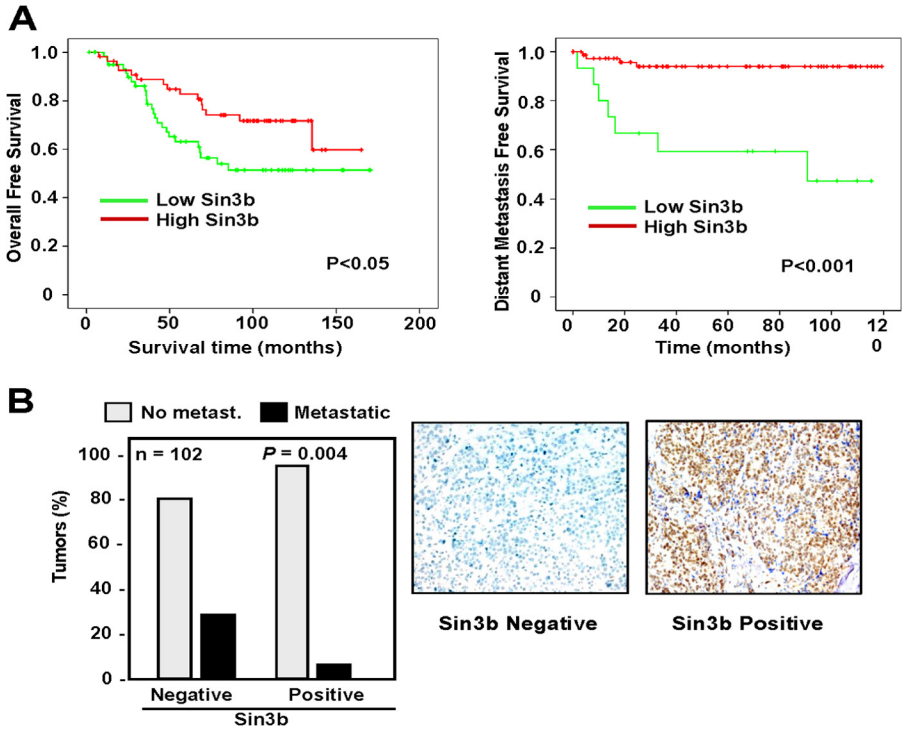

FIGURE 10. **Correlation of low Sin3b expression with poor survival in breast cancer.** *A*, correlation of Sin3b expression with Overall Free Survival and Distant Metastases Free Survival in human breast cancer. One data set of breast cancer and Sin3b expression (58) was used to generate Kaplan-Meier plots to show the correlation of Sin3b expression with overall free survival (*left*) and distant metastases free survival (*right*). *B*, representation of the correlation between Sin3b immunohistochemical expression and metastasis in invasive ductal breast carcinomas (*n*, number of tumors analyzed; *P*, statistical significance). Representative examples of the immunohistochemical study with and without expression of Sin3b are shown at the *right* (*scale*: ×200).

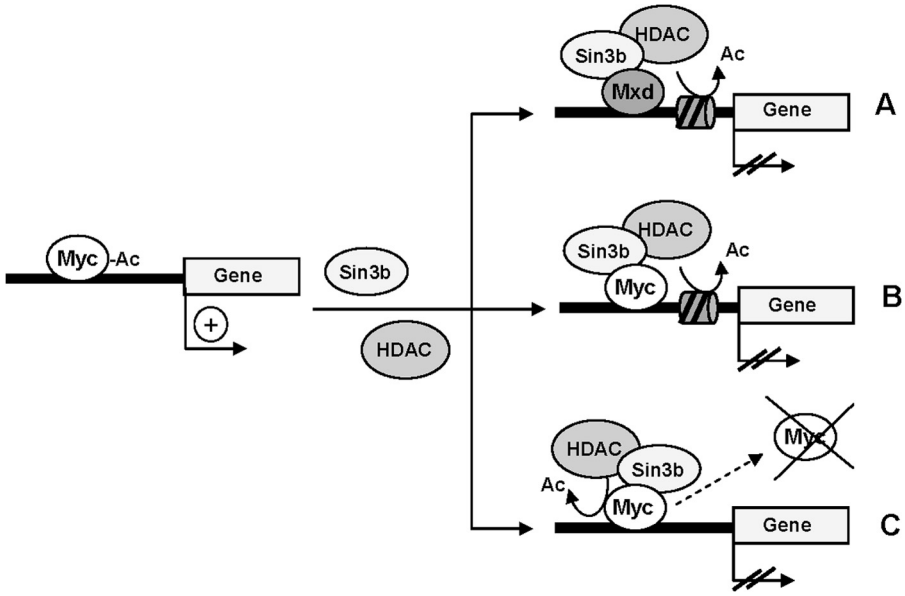

FIGURE 11. **Mechanistic models for Sin3b-Myc functional interaction.** The three mechanisms are not mutually exclusive. *A* and *B* show the already known activities of Sin3b. An additional mechanism, *C*, is favored in this study. In this mechanism, Sin3b recruits deacetylases, which would render the Myc protein more unstable. Other proteins in the Sin3b complex are not shown for simplicity. See "Discussion" for details.

binding. Therefore, we propose that Sin3 mediates the interaction of Myc with HDAC1, although interaction with other protein deacetylases cannot be ruled out. This proposal is based on these findings: (*a*) the co-expression of HDAC and Sin3b enhanced the repressive effect on E-box-containing reporters; (*b*) HDAC inhibitors (*e.g.* TSA and vorinostat) impaired the effect of Sin3b on Myc-mediated transcription; and (*c*) overexpression of HDAC alone did not modify Myc transcriptional activity. Therefore, Sin3b acts as a negative modulator of Myc transcriptional activity.

Several concomitant mechanisms could explain the repression of Myc activities by Sin3b. One would be the recruitment of Mxd protein to the promoter to exert transcriptional repression. This model is depicted in Fig. 11*A*. Although this mecha-

nism must operate *in vivo*, by itself it cannot explain our results, as the D186–203 Myc mutant did not interact with Sin3b and yet transactivated an E-box reporter even when Sin3b was co-expressed. Thus, the increase in Mxd-Sin3b-HDAC complexes on chromatin was not the main mechanism responsible for the diminished transcriptional activity of Myc in the presence of Sin3b.

A second explanation would be that the effect of Sin3b depends on histone deacetylation in the regulatory region of Myc-bound genes, leading to transcription repression (schematized in Fig. 11*B*). However, our ChIP results argue against this hypothesis as the major mechanism. In human leukemia cells, we found that both Myc and Sin3b bound to some promoters regardless of whether the gene was induced or repressed (Fig. 7), and Sin3b binding at these sites was not related to histone acetylation marks (48). Also, the combined analysis of ChIP-seq and RNA-seq data generated by the ENCODE consortium revealed that in K562 cells, the coincidence of Myc and Sin3a on the proximal promoters did not correlate with a lower expression with respect to genes with Myc alone (Fig. 8). Thus, our data do not support a direct role of Sin3b in transcriptional repression of Myc target genes. Given that the binding of Myc and Sin3b to chromatin can be transient, we cannot rule out an effect of Sin3b binding to Myc that leads to gene repression via histone deacetylation. Actually, Myc-mediated repression of some genes (*e.g. GADD45* and *ID2*) in Rat1a cells was impaired by co-transfection of Sin3b siRNA (not shown). However, taken together, the ChIP data are not consistent with this mechanism being the major one responsible for the decrease in Myc activity when Sin3b is co-expressed.

A third explanation is that Sin3b leads to reduced Myc levels. It is reported that Sin3a induces Myc deacetylation (53), and we have confirmed the same effect for Sin3b. Although the underlying mechanisms are not clear yet, it has been reported that acetylation of Myc by acetyltransferases (*e.g.* GCN5, Tip60, and p300/CBP) usually results in an increase in protein stability (49–53), although Myc deacetylation by Sirt1 results in increased stability (52). We showed that Sin3b decreased Myc levels, whereas Sin3b depletion augmented Myc levels. The simplest explanation is that Sin3b interaction contributes to Myc deacetylation leading to reduced Myc levels, as schematized in Fig. 11*C*. In agreement with the findings in cultured cells, we also found an association between high Sin3b and low Myc in human breast cancer samples (although the data were not statistically significant). In summary, the data suggest that, at least in some cell types, Sin3b controls Myc levels through a mechanism that involves protein deacetylation and destabilization. Further work is required to dissect the underlying mechanisms. On the other hand, transcriptional repression by Mxd of Myc target genes can also be mediated by Sin3b. Thus, Sin3b may reduce Myc activity through two parallel pathways: the canonical Sin3b-Mxd interaction, resulting in Myc target gene repression, and the reduction of Myc levels, as shown in this work. The effect of Sin3b on Myc activity opens possibilities of therapeutic intervention for Myc-driven tumors.

Acknowledgments—We are grateful to Bruno Amati, Amparo Cano, Luciano di Croce, Chi Dang, Gregory David, Robert N. Eisenman, Michaela Frye, and Simon Halegoua for reagents and comments and to Rosa Blanco and Pilar Frade for expert technical assistance.

REFERENCES

1. Meyer, N., and Penn, L. Z. (2008) Reflecting on 25 years with MYC. *Nat. Rev. Cancer* **8,** 976–990
2. Dang, C. V. (2012) MYC on the path to cancer. *Cell* **149,** 22–35
3. Conacci-Sorrell, M., McFerrin, L., and Eisenman, R. N. (2014) An overview of MYC and its interactome. *Cold Spring Harb. Perspect. Med.* **4,** a014357
4. Zeller, K. I., Zhao, X., Lee, C. W., Chiu, K. P., Yao, F., Yustein, J. T., Ooi, H. S., Orlov, Y. L., Shahab, A., Yong, H. C., Fu, Y., Weng, Z., Kuznetsov, V. A., Sung, W. K., Ruan, Y., Dang, C. V., and Wei, C. L. (2006) Global mapping of c-Myc binding sites and target gene networks in human B cells. *Proc. Natl. Acad. Sci. U.S.A.* **103,** 17834–17839
5. Orian, A., van Steensel, B., Delrow, J., Bussemaker, H. J., Li, L., Sawado, T., Williams, E., Loo, L. W., Cowley, S. M., Yost, C., Pierce, S., Edgar, B. A., Parkhurst, S. M., and Eisenman, R. N. (2003) Genomic binding by the *Drosophila* Myc, Max, Mad/Mnt transcription factor network. *Genes Dev.* **17,** 1101–1114
6. Li, Z., Van Calcar, S., Qu, C., Cavenee, W. K., Zhang, M. Q., and Ren, B. (2003) A global transcriptional regulatory role for c-Myc in Burkitt's lymphoma cells. *Proc. Natl. Acad. Sci. U.S.A.* **100,** 8164–8169
7. Fernandez, P. C., Frank, S. R., Wang, L., Schroeder, M., Liu, S., Greene, J., Cocito, A., and Amati, B. (2003) Genomic targets of the human c-Myc protein. *Genes Dev.* **17,** 1115–1129
8. Nie, Z., Hu, G., Wei, G., Cui, K., Yamane, A., Resch, W., Wang, R., Green, D. R., Tessarollo, L., Casellas, R., Zhao, K., and Levens, D. (2012) c-Myc is a universal amplifier of expressed genes in lymphocytes and embryonic stem cells. *Cell* **151,** 68–79
9. Lin, C. Y., Lovén, J., Rahl, P. B., Paranal, R. M., Burge, C. B., Bradner, J. E., Lee, T. I., and Young, R. A. (2012) Transcriptional amplification in tumor cells with elevated c-Myc. *Cell* **151,** 56–67
10. Eilers, M., and Eisenman, R. N. (2008) Myc's broad reach. *Genes Dev.* **22,** 2755–2766
11. Patel, J. H., Loboda, A. P., Showe, M. K., Showe, L. C., and McMahon, S. B. (2004) Analysis of genomic targets reveals complex functions of MYC. *Nat. Rev. Cancer* **4,** 562–568
12. Dang, C. V., O'Donnell, K. A., Zeller, K. I., Nguyen, T., Osthus, R. C., and Li, F. (2006) The c-Myc target gene network. *Semin. Cancer Biol.* **16,** 253–264
13. Leon, J., Ferrandiz, N., Acosta, J. C., and Delgado, M. D. (2009) Inhibition of cell differentiation: a critical mechanism for MYC-mediated carcinogenesis? *Cell Cycle* **8,** 1148–1157
14. Nesbit, C. E., Tersak, J. M., and Prochownik, E. V. (1999) MYC oncogenes and human neoplastic disease. *Oncogene* **18,** 3004–3016
15. Vita, M., and Henriksson, M. (2006) The Myc oncoprotein as a therapeutic target for human cancer. *Semin. Cancer Biol.* **16,** 318–330
16. Delgado, M. D., and León, J. (2010) Myc roles in hematopoiesis and leukemia. *Genes Cancer* **1,** 605–616
17. Hurlin, P. J., and Huang, J. (2006) The MAX-interacting transcription factor network. *Semin. Cancer Biol.* **16,** 265–274
18. Rottmann, S., and Lüscher, B. (2006) The Mad side of the Max network: antagonizing the function of Myc and more. *Curr. Top. Microbiol. Immunol.* **302,** 63–122
19. Grzenda, A., Lomberk, G., Zhang, J. S., and Urrutia, R. (2009) Sin3: master scaffold and transcriptional corepressor. *Biochim. Biophys. Acta* **1789,** 443–450
20. Grandinetti, K. B., and David, G. (2008) Sin3B: an essential regulator of chromatin modifications at E2F target promoters during cell cycle withdrawal. *Cell Cycle* **7,** 1550–1554
21. Ayer, D. E., Lawrence, Q. A., and Eisenman, R. N. (1995) Mad-Max transcriptional repression is mediated by ternary complex formation with mammalian homologs of yeast repressor Sin3. *Cell* **80,** 767–776

22. Laherty, C. D., Yang, W. M., Sun, J. M., Davie, J. R., Seto, E., and Eisenman, R. N. (1997) Histone deacetylases associated with the mSin3 corepressor mediate Mad transcriptional repression. *Cell* **89,** 349–356
23. Alland, L., Muhle, R., Hou, H., Jr., Potes, J., Chin, L., Schreiber-Agus, N., and DePinho, R. A. (1997) Role for N-CoR and histone deacetylase in Sin3-mediated transcriptional repression. *Nature* **387,** 49–55
24. Swanson, K. A., Knoepfler, P. S., Huang, K., Kang, R. S., Cowley, S. M., Laherty, C. D., Eisenman, R. N., and Radhakrishnan, I. (2004) HBP1 and Mad1 repressors bind the Sin3 corepressor PAH2 domain with opposite helical orientations. *Nat. Struct. Mol. Biol.* **11,** 738–746
25. Ayer, D. E., Laherty, C. D., Lawrence, Q. A., Armstrong, A. P., and Eisenman, R. N. (1996) Mad proteins contain a dominant transcription repression domain. *Mol. Cell. Biol.* **16,** 5772–5781
26. Heinzel, T., Lavinsky, R. M., Mullen, T. M., Söderstrom, M., Laherty, C. D., Torchia, J., Yang, W. M., Brard, G., Ngo, S. D., Davie, J. R., Seto, E., Eisenman, R. N., Rose, D. W., Glass, C. K., and Rosenfeld, M. G. (1997) A complex containing N-CoR, mSin3 and histone deacetylase mediates transcriptional repression. *Nature* **387,** 43–48
27. Rao, G., Alland, L., Guida, P., Schreiber-Agus, N., Chen, K., Chin, L., Rochelle, J. M., Seldin, M. F., Skoultchi, A. I., and DePinho, R. A. (1996) Mouse Sin3A interacts with and can functionally substitute for the amino-terminal repression of the Myc antagonist Mxi1. *Oncogene* **12,** 1165–1172
28. Gibbons, R. J. (2005) Histone modifying and chromatin remodelling enzymes in cancer and dysplastic syndromes. *Hum. Mol. Genet.* **14,** R85–R92
29. Cunliffe, V. T. (2008) Eloquent silence: developmental functions of Class I histone deacetylases. *Curr. Opin. Genet. Dev.* **18,** 404–410
30. Kouzarides, T. (2007) Chromatin modifications and their function. *Cell* **128,** 693–705
31. Silverstein, R. A., and Ekwall, K. (2005) Sin3: a flexible regulator of global gene expression and genome stability. *Curr. Genet.* **47,** 1–17
32. Nagy, L., Kao, H. Y., Chakravarti, D., Lin, R. J., Hassig, C. A., Ayer, D. E., Schreiber, S. L., and Evans, R. M. (1997) Nuclear receptor repression mediated by a complex containing SMRT, mSin3A, and histone deacetylase. *Cell* **89,** 373–380
33. Rayman, J. B., Takahashi, Y., Indjeian, V. B., Dannenberg, J. H., Catchpole, S., Watson, R. J., te Riele, H., and Dynlacht, B. D. (2002) E2F mediates cell cycle-dependent transcriptional repression in vivo by recruitment of an HDAC1/mSin3B corepressor complex. *Genes Dev.* **16,** 933–947
34. Xu, Y., Sengupta, P. K., Seto, E., and Smith, B. D. (2006) Regulatory factor for X-box family proteins differentially interact with histone deacetylases to repress collagen α2(I) gene (COL1A2) expression. *J. Biol. Chem.* **281,** 9260–9270
35. David, G., Grandinetti, K. B., Finnerty, P. M., Simpson, N., Chu, G. C., and Depinho, R. A. (2008) Specific requirement of the chromatin modifier mSin3B in cell cycle exit and cellular differentiation. *Proc. Natl. Acad. Sci. U.S.A.* **105,** 4168–4172
36. Mauleon, I., Lombard, M. N., Muñoz-Alonso, M. J., Cañelles, M., and Leon, J. (2004) Kinetics of Myc-Max-Mad gene expression during hepatocyte proliferation *in vivo*: differential regulation of Mad family and stress-mediated induction of c-Myc. *Mol. Carcinog.* **39,** 85–90
37. Schuhmacher, M., Staege, M. S., Pajic, A., Polack, A., Weidle, U. H., Bornkamm, G. W., Eick, D., and Kohlhuber, F. (1999) Control of cell growth by c-Myc in the absence of cell division. *Curr. Biol.* **9,** 1255–1258
38. Hoang, A. T., Lutterbach, B., Lewis, B. C., Yano, T., Chou, T. Y., Barrett, J. F., Raffeld, M., Hann, S. R., and Dang, C. V. (1995) A link between increased transforming activity of lymphoma-derived MYC mutant alleles, their defective regulation by p107, and altered phosphorylation of the c-Myc transactivation domain. *Mol. Cell. Biol.* **15,** 4031–4042
39. Vaqué, J. P., Fernández-García, B., García-Sanz, P., Ferrandiz, N., Bretones, G., Calvo, F., Crespo, P., Marín, M. C., and León, J. (2008) c-Myc inhibits Ras-mediated differentiation of pheochromocytoma cells by blocking c-Jun up-regulation. *Mol. Cancer Res.* **6,** 325–339
40. Gómez-Casares, M. T., García-Alegria, E., López-Jorge, C. E., Ferrándiz, N., Blanco, R., Alvarez, S., Vaqué, J. P., Bretones, G., Caraballo, J. M., Sánchez-Bailón, P., Delgado, M. D., Martín-Perez, J., Cigudosa, J. C., and León, J. (2013) MYC antagonizes the differentiation induced by imatinib in chronic myeloid leukemia cells through downregulation of p27(KIP1.). *Oncogene* **32,** 2239–2246
41. Blackwood, E. M., and Eisenman, R. N. (1991) Max: a helix-loop-helix zipper protein that forms a sequence-specific DNA-binding complex with Myc. *Science* **251,** 1211–1217
42. Kiessling, A., Sperl, B., Hollis, A., Eick, D., and Berg, T. (2006) Selective inhibition of c-Myc/Max dimerization and DNA binding by small molecules. *Chem. Biol.* **13,** 745–751
43. Söderberg, O., Gullberg, M., Jarvius, M., Ridderstråle, K., Leuchowius, K. J., Jarvius, J., Wester, K., Hydbring, P., Bahram, F., Larsson, L. G., and Landegren, U. (2006) Direct observation of individual endogenous protein complexes *in situ* by proximity ligation. *Nat. Methods* **3,** 995–1000
44. Quinlan, A. R., and Hall, I. M. (2010) BEDTools: a flexible suite of utilities for comparing genomic features. *Bioinformatics* **26,** 841–842
45. Delgado, M. D., Lerga, A., Cañelles, M., Gómez-Casares, M. T., and León, J. (1995) Differential regulation of Max and role of c-Myc during erythroid and myelomonocytic differentiation of K562 cells. *Oncogene* **10,** 1659–1665
46. Weibrecht, I., Leuchowius, K. J., Clausson, C. M., Conze, T., Jarvius, M., Howell, W. M., Kamali-Moghaddam, M., and Söderberg, O. (2010) Proximity ligation assays: a recent addition to the proteomics toolbox. *Expert Rev. Proteomics* **7,** 401–409
47. Hopewell, R., and Ziff, E. B. (1995) The nerve growth factor-responsive PC12 cell line does not express the Myc dimerization partner Max. *Mol. Cell. Biol.* **15,** 3470–3478
48. Martinato, F., Cesaroni, M., Amati, B., and Guccione, E. (2008) Analysis of Myc-induced histone modifications on target chromatin. *PLoS ONE* **3,** e3650
49. Vervoorts, J., Lüscher-Firzlaff, J. M., Rottmann, S., Lilischkis, R., Walsemann, G., Dohmann, K., Austen, M., and Lüscher, B. (2003) Stimulation of c-MYC transcriptional activity and acetylation by recruitment of the cofactor CBP. *EMBO Rep.* **4,** 484–490
50. Patel, J. H., Du, Y., Ard, P. G., Phillips, C., Carella, B., Chen, C. J., Rakowski, C., Chatterjee, C., Lieberman, P. M., Lane, W. S., Blobel, G. A., and McMahon, S. B. (2004) The c-MYC oncoprotein is a substrate of the acetyltransferases hGCN5/PCAF and TIP60. *Mol. Cell. Biol.* **24,** 10826–10834
51. Faiola, F., Liu, X., Lo, S., Pan, S., Zhang, K., Lymar, E., Farina, A., and Martinez, E. (2005) Dual regulation of c-Myc by p300 via acetylation-dependent control of Myc protein turnover and coactivation of Myc-induced transcription. *Mol. Cell. Biol.* **25,** 10220–10234
52. Menssen, A., Hydbring, P., Kapelle, K., Vervoorts, J., Diebold, J., Lüscher, B., Larsson, L. G., and Hermeking, H. (2012) The c-MYC oncoprotein, the NAMPT enzyme, the SIRT1-inhibitor DBC1, and the SIRT1 deacetylase form a positive feedback loop. *Proc. Natl. Acad. Sci. U.S.A.* **109,** E187–E196
53. Nascimento, E. M., Cox, C. L., MacArthur, S., Hussain, S., Trotter, M., Blanco, S., Suraj, M., Nichols, J., Kübler, B., Benitah, S. A., Hendrich, B., Odom, D. T., and Frye, M. (2011) The opposing transcriptional functions of Sin3a and c-Myc are required to maintain tissue homeostasis. *Nat. Cell Biol.* **13,** 1395–1405
54. Grandinetti, K. B., Jelinic, P., DiMauro, T., Pellegrino, J., Fernández Rodríguez, R., Finnerty, P. M., Ruoff, R., Bardeesy, N., Logan, S. K., and David, G. (2009) Sin3B expression is required for cellular senescence and is upregulated upon oncogenic stress. *Cancer Res.* **69,** 6430–6437
55. Le Guezennec, X., Vermeulen, M., and Stunnenberg, H. G. (2006) Molecular characterization of Sin3 PAH-domain interactor specificity and identification of PAH partners. *Nucleic Acids Res.* **34,** 3929–3937
56. Herbst, A., Hemann, M. T., Tworkowski, K. A., Salghetti, S. E., Lowe, S. W., and Tansey, W. P. (2005) A conserved element in Myc that negatively regulates its proapoptotic activity. *EMBO Rep.* **6,** 177–183
57. Kurland, J. F., and Tansey, W. P. (2008) Myc-mediated transcriptional repression by recruitment of histone deacetylase. *Cancer Res.* **68,** 3624–3629
58. Chin, K., DeVries, S., Fridlyand, J., Spellman, P. T., Roydasgupta, R., Kuo, W. L., Lapuk, A., Neve, R. M., Qian, Z., Ryder, T., Chen, F., Feiler, H., Tokuyasu, T., Kingsley, C., Dairkee, S., Meng, Z., Chew, K., Pinkel, D., Jain, A., Ljung, B. M., Esserman, L., Albertson, D. G., Waldman, F. M., and Gray,

J. W. (2006) Genomic and transcriptional aberrations linked to breast cancer pathophysiologies. *Cancer Cell* **10,** 529–541

59. van de Vijver, M. J., He, Y. D., van't Veer, L. J., Dai, H., Hart, A. A., Voskuil, D. W., Schreiber, G. J., Peterse, J. L., Roberts, C., Marton, M. J., Parrish, M., Atsma, D., Witteveen, A., Glas, A., Delahaye, L., van der Velde, T., Bartelink, H., Rodenhuis, S., Rutgers, E. T., Friend, S. H., and Bernards, R. (2002) A gene-expression signature as a predictor of survival in breast cancer. *N. Engl. J. Med.* **347,** 1999–2009
60. Perreard, L., Fan, C., Quackenbush, J. F., Mullins, M., Gauthier, N. P., Nelson, E., Mone, M., Hansen, H., Buys, S. S., Rasmussen, K., Orrico, A. R., Dreher, D., Walters, R., Parker, J., Hu, Z., He, X., Palazzo, J. P., Olopade, O. I., Szabo, A., Perou, C. M., and Bernard, P. S. (2006) Classification and risk stratification of invasive breast carcinomas using a real-time quantitative RT-PCR assay. *Breast Cancer Res.* **8,** R23